TITLE PAGE

COSMIC RAYS VARIABILITY IN THE MID AND HIGH LATITUDES DURING SOLAR QUIET DAYS

BY

OKIYI, MIRACLE UGOCHUKWU

(UNN/PG/M.Sc./14/68235)

A PROJECT WORK PRESENTED TO THE DEPARTMENT OF PHYSICS AND ASTRONOMY OF THE FACULTY OF PHYSICAL SCIENCES, UNIVERSITY OF NIGERIA, NSUKKA IN PARTIAL FULFILMENT FOR THE AWARD OF MASTER OF SCIENCE (M.Sc.) IN SPACE SCIENCE, (ATMOSPHERIC PHYSICS).

SUPERVISOR: DR. K.C OKPALA

SEPTEMBER, 2016.

APPROVAL PAGE

This is to certify that the project topic **"cosmic rays variability at mid and high latitudes during solar quiet days"** was approved as a research work for the award of Master of Science (M.Sc) in space science (Atmospheric physics).

SUPERVISOR DATE SIGNATURE
DR. OKPALA, K. C.

HEAD OF DEPARTMENT DATE SIGNATURE
PROFESSOR EKWEALOR A. B. C.

EXTERNAL EXAMINER --

DATE SIGNATURE

CERTIFICATION

This is to certify that the work expressed in this project is the original topic assigned to the researcher for the certificate of Master of Science (M.Sc) degree in the Department of Physics and Astronomy.

Okiyi Miracle Ugochukwu

UNN/PG/M.Sc/2014/68235

DEDICATION

This project work is dedicated to God Almighty for His infinite mercy and to every member of my family and friends for their immeasurable contributions in my life.

ACKNOWLEDGEMENT

Firstly, I will like to thank my supervisor Dr. K.C Okpala of the Department of Physics and Astronomy, University of Nigeria, Nsukka. His door was always open whenever I ran into a trouble spot or had a question about my research or writing. He consistently allowed this project to be my own work, but steered me in the right direction whenever he thought I needed it.

I will also like to thank members of the Atmospheric and Geophysics Research Group (AGRG) of UNN. Without their passionate participation and input, the project could not have been successfully conducted.

I will also like to acknowledge Dr. E.B.I. Ugwu of the Department of Physics and Astronomy, University of Nigeria, Nsukka, who was the discussant of this work during my M.Sc presentation. I am gratefully indebted to him for his very valuable comments.

Finally, I must express my very profound gratitude to my parents Mr. and Mrs. B.C Okiyi, not also forgetting my best friend Ugoala, Marvelous Ugomma for providing me with unfailing support and continuous encouragement throughout my years of study. This accomplishment would not have been possible without them. Thank you.

ABSTRACT

We have studied the variability of Cosmic rays flux during solar quiet days at mid and high latitudes. By using the five (5) quietest days for each month, the monthly mean diurnal variation of cosmic ray anisotropy have been derived for the period 1981-2007, which covers part of cycles 21, 22 and 23. These quiet days are days during which the sun is relatively magnetically quiet, leading to less anisotropic behavior in the diurnal flux of cosmic rays measured on the earthꞌs surface. Four stations (Rome, Oulu, Inuvik and Thule) were used in this study to understand the important features of the high latitude and mid-latitude diurnal wave, and how solar and geomagnetic activity may be influencing the wave characteristics. Cosmic ray wave characteristics were obtained by discrete Fourier transform (DFT). The mean, diurnal amplitude, phase and dispersion for each month's diurnal wave were calculated and profiled. There was clear indication that the terrestrial effect on the variability of the monthly mean was more associated with geomagnetic activity rather than rigidity of the cosmic rays. Correlation of the time series of these wave characteristics with solar and geomagnetic activity index showed better association with solar activity.

TABLE OF CONTENTS

LIST OF FIGURES

LIST OF TABLES

CHAPTER ONE

1.1 INTRODUCTION

Cosmic rays are high-energy charged particles originating mainly from the outer space. They travel at nearly the speed of light and strike the earth from all directions. Most cosmic rays are nuclei of atoms ranging from the lightest to the heaviest elements in the periodic table. Cosmic rays also include high energy electrons, positrons and other subatomic particles. There are broadly three types of cosmic rays; solar cosmic rays (SCRs), galactic cosmic rays (GCRs) and anomalous cosmic rays (ACRs). SCRs originate from the sun and have energy within the range (kilo-electron volt) KeV < 10 to 100 MeV (Mega-electron volt) occasionally reaching 1GeV (Giga-electron volt). GCRs originate from supernovae explosions. They have energy within the range 100MeV < E < 10GeV. ACRs originate from neutral interstellar atoms that have been ionized by solar UV radiation after entering the heliosphere. They have energies of 10^7 - 10^8 eV. Cosmic rays attract great interest due to the damage they inflict on electronics and life outside the protection of an atmosphere and a magnetic field, they also provide important channels for astrophysical information.

1.2 DISCOVERY AND EARLY RESEARCH

Cosmic rays were discovered in 1912 by Victor Hess when he found that an electroscope discharged more rapidly as he ascended in a balloon. He attributed this to a source of radiation entering the atmosphere from above and in 1936 was awarded a noble prize in physics for his discovery. For some time it was believed that the radiation was electromagnetic in nature (hence the name cosmic ñrayò) and some textbooks still incorrectly include cosmic rays as part of the electromagnetic spectrum. However, during the 1930ôs it was found that cosmic rays must be electrically charged because they are affected by the earthôs magnetic field.

From the 1930s to the 1950s before man-made particle accelerators reached very high energies, cosmic rays served as source of particles for high energy physics investigations which led to the discovery of subatomic particles that included the positron and muon. Some of these applications have continued ever with the dawn of space age. The main focus of cosmic ray research has been directed towards astrophysical investigations of where cosmic rays originate, how they get accelerated to such high velocities, what role they play in the dynamics of the galaxy and what their composition tells us about matter from outside the solar system. To measure cosmic rays count rate before they have been slowed down and broken up by the atmosphere, research is carried out by instruments mounted on spacecraft and high altitude balloons, using particle detectors similar to those used in nuclear and high energy physics experiments.

1.3 COSMIC RAY COMPOSITION

Cosmic rays include essentially all of the elements in the periodic table; about 89% of the nuclei are hydrogen (protons), 10% helium and about 1% other heavier elements. The common heavier elements (such as carbon, oxygen, magnesium, silicon and iron) are present in similar relative abundances as in the solar system but there are important differences in elemental and isotopic composition that provide information on the origin and history of galactic cosmic rays. For example, there is a significant overabundance of the rare elements Li, Be and B produced when heavier cosmic rays such as carbon, nitrogen and oxygen disintegrate into lighter nuclei during collisions with the interstellar gas. The isotope ^{22}Ne is also overabundant, showing that the nucleosynthesis of cosmic rays and solar system material differ.

1.4 COSMIC RAYS IN THE SOLAR SYSTEM

Just as cosmic rays are deflected by the magnetic field in interstellar space, they are also affected by the interplanetary magnetic field embedded in the solar wind (the plasma of ions and electrons blowing from the solar corona at about 400km/sec) and therefore have difficulty reaching the inner solar system. Spacecrafts (e.g. voyager 1 and 2) venturing out towards the boundary of the solar system has found that the intensity of galactic cosmic rays increases with distance from the sun. As solar activity varies over the 11-year solar cycle the intensity of cosmic rays at Earth also varies in anti-correlation with the sunspot number.

The sun is also a sporadic source of cosmic ray nuclei and electrons that are accelerated by shock waves traveling through the corona as solar flares thereby releasing magnetic energy; during such occurrences, the intensity of energetic particles in space can increase by a factor of 10^2 to 10^6. Such solar particle events are much more frequent during the active phase of the solar cycle. The maximum energy reached in solar particle events is typically 10 to 100MeV, occasionally reaching 1GeV (approximately once a year) to 10GeV (approximately once a decade). Solar energetic particles can be used to measure the elemental and isotopic composition of the sun, thereby complementing spectroscopic studies of solar material.

1.5 COSMIC RAYS ON EARTH

When high energy cosmic rays undergo collisions with atoms of the upper atmosphere, they produce a cascade of ñsecondaryò particles that shower down through the atmosphere to the earthôs surface. Secondary cosmic rays include pions (which quickly decay to produce muons, neutrinos and gamma rays), as well as electrons and positrons produced by muon decay and gamma ray interaction with atmospheric atoms. The number of particles reaching the Earthôs surface is directly related to the energy of the cosmic ray that strikes the upper atmosphere as low energy cosmic rays are blocked off by the atmosphere. Cosmic rays with energies beyond 10^{14}eV are studied with large ñair showerò arrays of detectors distributed over many square kilometres that sample the particles produced. The frequency of air showers ranges from about

100 per m^2 for a year with energies > 10^{15}eV to only about 1 per km^2 for a century with energies beyond 10^{20}eV. Cosmic ray interaction products such as neutrinos are also studied by large detectors placed deep in underground mines or underwater, see figure 1.

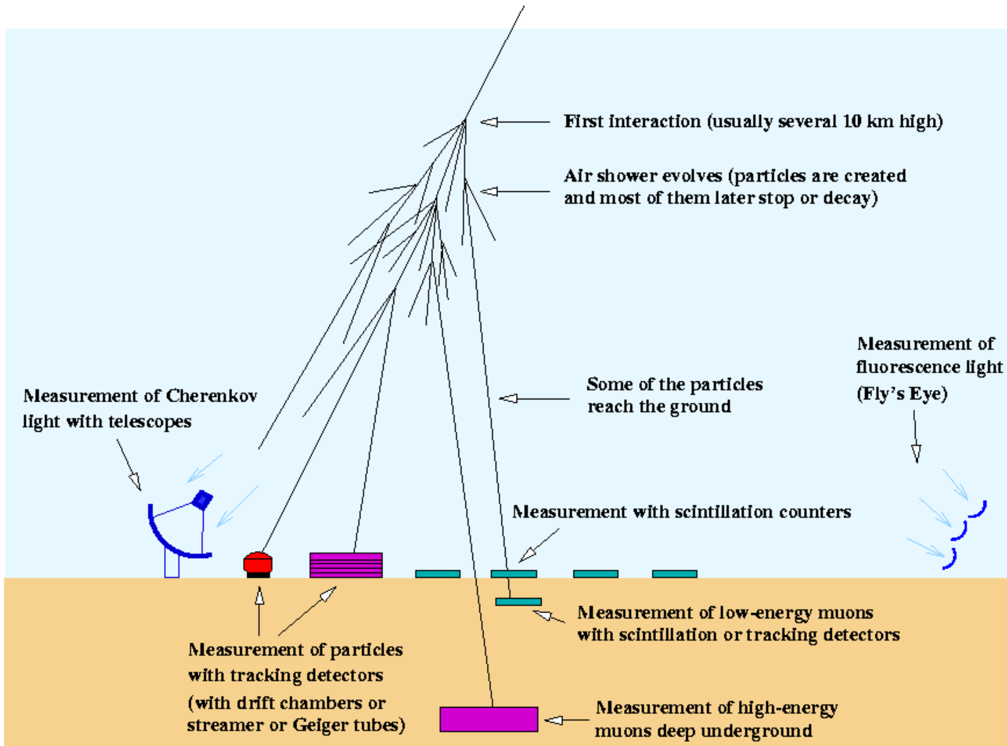

Figure 1: Air shower array created when cosmic rays impinge on the atmosphere. (http://en.m.wikipedia.org/wiki/cosmic-ray observatory)

Most secondary cosmic rays reaching the earthôs surface are muons with an average of about 100 per m^2 for a second. Although, thousands of cosmic rays pass through our bodies every minute, the resulting radiation levels are relatively low, corresponding to only a few percent of the natural background radiation. However, the greater intensity of cosmic rays in outer space is a potential radiation hazard for astronauts, especially when the sun is active and interplanetary space may suddenly be filled with solar energetic particles. Cosmic rays are also a hazard to electronic instruments in space; impacts of heavily ionizing cosmic ray nuclei can cause computer memory bits to ñflipò or microcircuit to fail.

Cosmic rays are also responsible for the continuous production of a number of unstable isotopes in the Earthôs atmosphere, such as carbon-14 through the reaction;

$$n \quad + \quad N^{14} \quad \rightarrow \quad P \quad + \quad C^{14}$$

It is not uncommon for cosmic rays to collide with atoms in the atmosphere, creating secondary cosmic ray in the form of an energetic neutron and for these energetic neutrons to collide with nitrogen atoms. When the neutron collides, a nitrogen-14 (seven protons, seven neutrons) atom turns into a carbon-14 atom (six protons, eight neutrons) and a hydrogen atom. Cosmic rays kept the level of carbon-14 in the atmosphere fairly constant (70 tons) for at least the past 100,000 years, until the beginning of above-ground nuclear weapons testing in the early 1950s.

The earthôs atmosphere shields us from cosmic rays radiation, exposure increases as altitude increases; the exposure at aircraft altitudes is about 100 times greater than on the ground. The difference in shielding between high and low latitude has a much more marked effect on exposure at aircraft altitudes than at the surface. At 50^o, exposure is up to 4 times greater than at the equator.

1.6 COSMIC RAY VARIABILITY

Cosmic ray (CR) variability is a complex phenomenon which occurs all over the heliosphere and depends on many factors. No single solar index, however sophisticated can account for cosmic ray variations (Helen and Evangelos, 2012). Different scientists proposed empirical relations describing the long-term cosmic ray variations based on the joint use of solar and/or heliospheric indices. At first, solar indices such as sunspot number and solar flares were used; later Belov *et al*. (1999) proposed a multi-parametric description of long-term cosmic ray variations. The flux (count rate) of cosmic rays incident on the earthĝs upper atmosphere is varied by two processes; solar wind and earthĝs magnetic field.

Solar wind purges out magnetized plasma generated by the sun and this decelerates incoming particles as well as excluding some of the particles with energies below about 1GeV (Figure 2). The amount of solar wind is not constant due to changes in solar activities; hence the level of variation changes with solar activity.

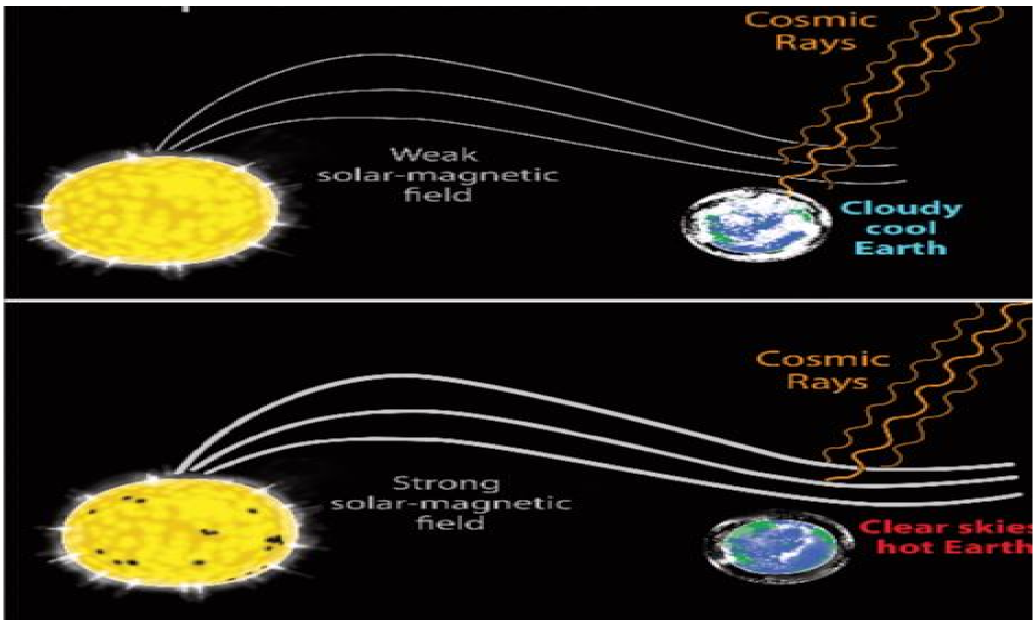

Figure 2: Solar wind modulation of cosmic rays (https:ktwop.com/tag/henrik-svensmark)

The cosmic flux varies from the eastern and western directions due to the polarity of the Earthĝs geomagnetic field and the positive charge dominance in primary cosmic rays (east-west effect). The cosmic ray intensity at the equator is lower than that at the poles as the geomagnetic cut-off value is greatest at the equator; this is because charged particles tend to move in the direction of field lines and not across them so that they are concentrated in the polar region.

The geomagnetic field modulates the CR flux through the cut-off rigidity which can be adequately described by Stormerĝs equation (Stormer, 1955):

$$P_C = 1.9M\left(\frac{R_0}{R}\right)^2 \cos^4 \lambda_G [GV].\qquad (1)$$

where M is the geomagnetic field dipole moment (in 10^{25} Gcm^3), R_o is the Earthôs mean radius, R is the distance from the given location to the dipole centre, and λ_G is the geomagnetic latitude. Generally, earthôs magnetic field consists of two main components

- The main field (origin is deep inside the earth)
- The variation field (source is from the upper atmosphere)

Geomagnetic variation includes spatial and temporal variations. As the name implies, spatial variation of the geomagnetic field is the modulation from place to place, while temporal variation of the geomagnetic field is the modulation of geomagnetic field from time to time. Figure 4 is an Organogram which illustrates the various temporal variation of the geomagnetic field of which the solar quiet day is one.

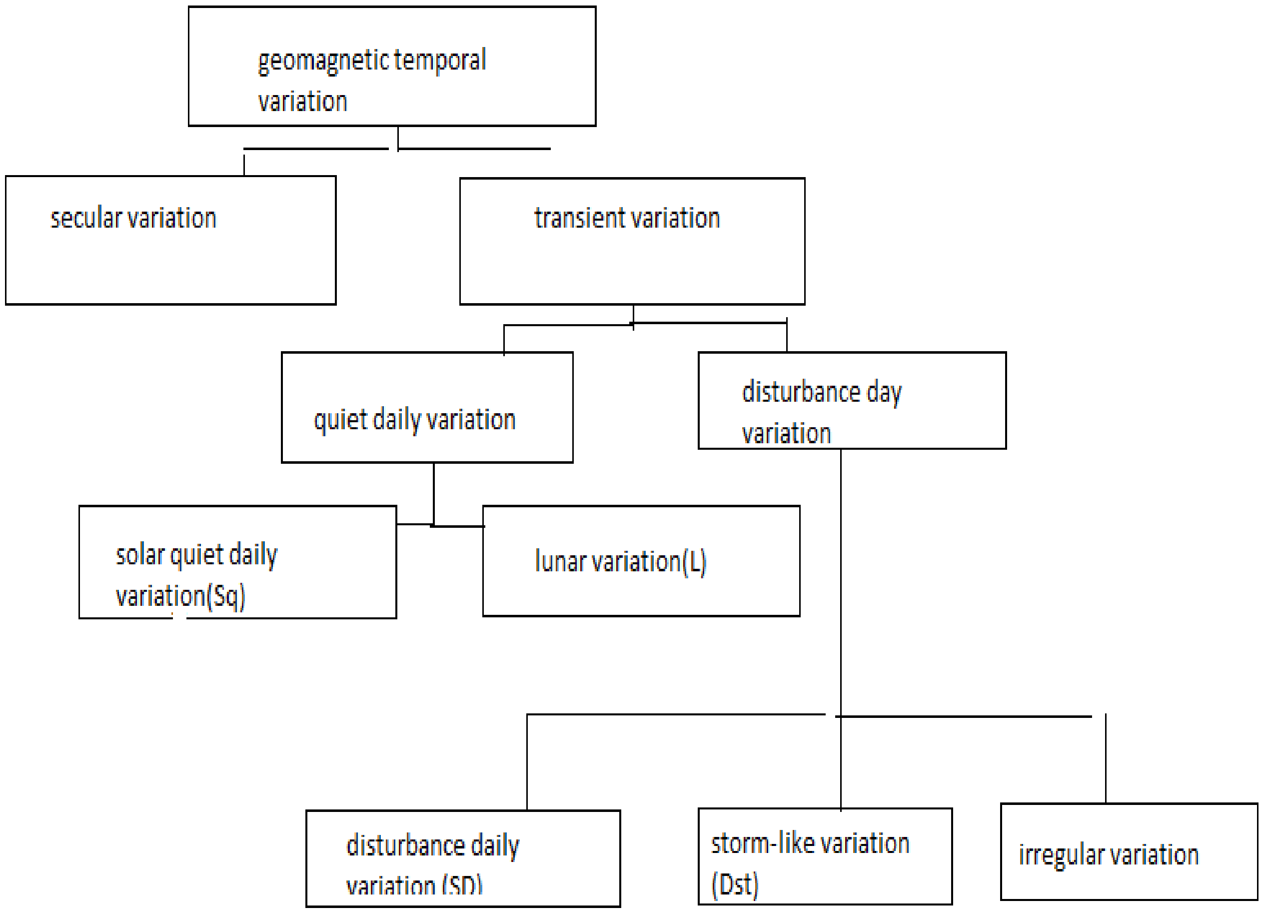

Figure 3: Organogram of geomagnetic temporal variations

1.7 SOLAR QUIET DAYS AND SOLAR ACTIVITY CYCLE

Solar quiet days refer to days when the sunǾs activity is minimal. These days are associated with little changes in the sunǾs magnetic field with few records of sunspots, coronal mass ejections and solar flares. The sunǾs activity varies on an 11-year cycle, typically taking about five and a half (5½) years to move from the quiet (solar minimum) to the more disturbed solar maximum. The solar cycle is determined by the changes in the number of dark splotches on the surface of the sun called sunspots and these short-lived patches are caused by intense magnetic activity. The frequency and number of these dark splotches on the sunǾs surface act as indicators of the sunǿs activity as it moves between solar minimum and solar maximum. Sunspots sometimes erupt into powerful solar storms that shoot streams of charged particles into space, occasionally in the direction of the Earth.

In the early 20th century, George Ellery Hale was first to show that the 11-year sunspot cycle was actually half of a 22-year magnetic cycle during which the polarity of the sunǿs magnetic field reverses from 11-year sunspot cycle to the next. The leading sunspot in each bipolar region exhibit magnetic north polarity while the following one exhibit the south magnetic polarity; this polarity is reversed after each cycle. The predominant theory for what causes this magnetic cycle involves a dynamics in the interior of the sun, such as the dynamo that generates the magnetic field of the planets (Hester *et al*., 2002).

1.8 EFFECTS OF COSMIC RAYS

The galactic cosmic rays (GCRs) originating from astrophysical sources and traversing through the interstellar/interplanetary medium reach the terrestrial atmosphere and produce complex dynamic changes in it. The flow rate of the GCRs incident in the earthǿs upper atmosphere is varied by the solar wind and the geomagnetic field. The effect of galactic cosmic rays include; Changes in Atmospheric Chemistry- Cosmic rays ionize the nitrogen and oxygen molecules in the atmosphere, which leads to a number of chemical reactions including ozone depletion. Ambient Radiation- Cosmic rays constitute a fraction of the annual radiation exposure of human beings on the earth, averaging 0.39mSv out of a total of 3mSv per year for the earthǿs population. However, the background radiation from cosmic rays increases with altitude, from 0.3mSv per year for sea-level areas to 1.0mSv per year for higher altitude cities. Airline crews flying long distance high altitude routes can be exposed to 2.2mSv of extra radiation each year due to cosmic rays nearly doubling their total ionizing radiation exposure.

Galactic cosmic rays are one of the barriers in prospective interplanetary travel by crewed spacecraft. Cosmic rays also pose a threat to electronics placed aboard outgoing probes. In 2010, a malfunction aboard the voyager 2 space probe was credited to a single flipped bit, probably caused by a cosmic ray. Strategies such as physical or magnetic shielding for spacecraft have been considered in order to minimize the damage to electronics and human beings caused by cosmic rays. The indirect radiative forcing of atmospheric aerosols is sensitive to particle size and concentration, which are influenced significantly by nucleation processes. Through its role in the aerosol formation, the cosmic ray may affect the cloud condensation nuclei abundance and hence the global cloud properties and climate. Systematic variations in ionization rates due to the modulation of cosmic ray radiation by the solar cycle are sufficient to cause notable variations in aerosol production. It has been found that the signs of such variations are altitude-dependent.

The role of cosmic rays directly or via solar-induced modulations in climate change was suggested by Edward. P. Ney in 1959 and by Robert. E. Dickinson in 1975. The idea has been revised in recent years. Svensmark (2007) has argued that because solar variations modulate the cosmic ray flux on earth, they will consequently affect the rate of cloud formation and climate. However, other scientists disagree. Most climate scientist support the conclusions of 2007 IPCC synthesis report which strongly attributes a major role in the ongoing global warming to human-produced gases such as carbon dioxide, methane, nitrous oxide. It also stated that models including natural forcing only (including aerosol forcing, which cosmic rays are considered by some to contribute to) would result in far less warming than has actually been observed or predicted in models including anthropogenic forcing.

1.8 PURPOSE OF STUDY

The purposes of this study is to investigate the cosmic rays variability in the mid and high latitudes during solar quiet days.

The following are the objectives of this study:

i. investigation of the features of temporal and spatial variability of mid and high latitude diurnal cosmic ray flux during quiet geomagnetic conditions.

ii. to determine if there is any association between quiet time cosmic ray variability and geomagnetic activity at mid and high latitudes.

iii. determine solar activity dependent features of the phase of cosmic rays diurnal variation.

CHAPTER TWO

LITERATURE REVIEW

2.1 INTRODUCTION

Cosmic rays play an important role in the solar system and galactic astrophysics. Many researchers have tried to understand the variability of cosmic ray because of their possible effects on geophysical processes. Cosmic ray (CR) count rates measured on Earth are affected by heliospheric and geomagnetic modulation in addition to atmospheric effects on the flux arriving from outside the heliosphere. The diurnal variation of cosmic rays is the result of a complex combination of the effects of the interplanetary magnetic field (IMF) and geomagnetic field in addition to latitude and altitude of the location of detection on Earth. The variability of cosmic ray flux on long term and short term basis has been studied extensively by quite a number of authors (Singer, 1952, Pomerantz and Duggal, 1971, Ananth *et al*., 1993, Okpala and Okeke, 2011, Bazilevskaya *et al.*, 1995, Usoskin and Kalevi, 2001, Kudela *et al*., 2008, Sabbah and Kudela, 2011, Singh and Badruddin, 2015). The diurnal variation of cosmic rays can be characterized by the maximal value (amplitude) and phase (time of the maximal amplitude) in addition to the mean dispersion of the diurnal flux from the harmonic signatures. The simple harmonic analysis of the diurnal variation of cosmic rays flux has been applied by many authors (Agarwal and Mishra, 2008, Kudela *et al.,* 2008, Kane, 2009, Sabbah and Kudela, 2011, Okpala and Okeke, 2011, Singh and Badruddin, 2015) and their linear association with different possible drivers has been investigated.

2.2 SOLAR MODULATION OF COSMIC RAY

As expected, the sun is a dominant contributor to diurnal cosmic ray flux and atmospheric effects are expected to play significant role in the seasonal variation (Pomerantz and Duggal, 1971).

Bazilevskaya *et al.* (1995) studied the relationship between the galactic cosmic ray intensity and the sunspot distribution. A satisfactory relationship was found between the solar activity index and the galactic cosmic ray (GCR) intensity over more than three 11-year cycles. The number of sunspot and mean heliolatitude (‶Ωū index) describe the GCR behaviour rather well. The good correlation between the time dependence of the heliolatitude (‶Ωū index) and the HCS tilt during 1983-1988 enabled Bazilevskaya *et al*. (1995) to infer that these parameters are controlled by the large-scale solar magnetic field. Tiwari *et al*. (2011) worked on the relationship of cosmic rays with solar activities. From their analysis, it was suggested that the modulation of galactic cosmic rays should have a significant component controlled by the state of the interplanetary magnetic fields as transported out from the sun and hence there should be a solar cycle effect on the drift of the cosmic rays in the heliosphere. They suggested that there were many mechanisms, which explain the long-term modulation process of cosmic rays. The drift due to the waviness of the neutral current sheet is one of the causes. The curvature of the solar magnetic field and Global Merged Interaction Region are the other causes of cosmic ray long-term modulation.

2.3 GEOMAGNETIC FIELD MODULATION OF COSMIC RAY

Shea and Smart (1990) were able to summarize how the geomagnetic field is used to calculate cosmic ray vertical rigidities and how this values are used as an ordering parameter for different cosmic radiation investigations. Shea and Smart (2004) also worked on Preliminary study of cosmic rays, geomagnetic field changes and possible climate changes. They noted that the average solar cycle modulation of the galactic cosmic radiation over the past four solar cycles has been ~8% in the equatorial regions and ~18% at high latitudes; in addition, there have been short-lived transient events when the modulation has been more than 25% at high latitudes. Okpala (2015) in his work on galactic cosmic ray variability at two neutron monitors: relation to

Kp index; stated that difference in the amplitude of galactic cosmic ray flux at Newark and Apatity neutron monitor stations depends on the level of interplanetary disturbance (Kp). The difference is highest during low Kp conditions and lowest during high Kp condition.

2.4 COSMIC RAY VARIABILITY AND PERIODICITY

Kudela *et al*. (2008) studied long term behaviour of the diurnal wave of cosmic ray anisotropy in relation with interplanetary magnetic field. Attempts to understand the cause and effects of the relationship between cosmic ray diurnal wave anisotropy and geomagnetic/interplanetary fields is still an active area of research (Sabbah and Kudela, 2011). Singh and Badruddin (2015) studied the short term oscillations (Ò1 solar cycle rotation) of the solar wind parameters, galactic cosmic rays and geomagnetic indices during the solar minimum between cycles 22/23 and 23/24. They reported 7.1 days, 5.5 days, 4.4 days and 3.3 days oscillations in solar wind parameters (IMF, Bz and Ey) and geomagnetic disturbance proxies (Dst and AE) during relatively quiet periods. These quasi periodicities are likely related to the period of solar wind structures bounded with the solar magnetic field polarity, IMF and solar wind characteristics (Sabbah, 2007). The complexity of the spatial structure of the interplanetary magnetic field (IMF) and its evolution within the heliosphere, in addition to the changes in the geomagnetic field, causes variability in contribution to the quasi-periodic variations in cosmic ray. The solar activity and solar magnetic field cyclicities contribution to the quasi periodicity of signals in CR is particularly important for long term studies (Kudela and Sabbah, 2016).

The different roles of the IMF on diurnal waves of cosmic rays during disturbed and quiet conditions are not well established. For instance, low energy galactic cosmic rays with energies below few tens of GeV are moving mostly along lines of IMF and their intensity should peak at time of best connections of solar magnetic field with geomagnetic field (Chillingarian and

Mailyan, 2009). During disturbed conditions, the evolution of the IMF is well studied and cosmic ray count rates are known to undergo established transient phenomena like ground level enhancements and Forbush effects. Studying the evolution of IMF during quiet condition is of importance for a better understanding of the effect of the IMF on the diurnal flux of cosmic rays. Firoz (2008) observed narrower distribution of IMF total magnetic field and its polarity during quiet days (when compared with disturbed days). In addition, the northward component of the IMF Bz tend to dominate during quiet period. This suggests that the quiet day distribution indicates periods of less powerful interplanetary shock waves as to affect the magnetic field of the earth.

The five international quiet days are believed to be better optimized for long term and short term studies of daily variation (Kumar *et al*., 1998). Since the variation of the IMF total magnetic field during quiet conditions is generally low, diurnal wave may likely be controlled by velocity component of the solar wind during quiet conditions. Firoz (2008) observed differences between days with low (quiet) and high (disturbed) diurnal waves of cosmic rays; they are characterized by differences in the distribution of phase. According to Kudela *et al.* (2008), the amplitude to average ratio is a useful parameter for understanding the diurnal wave contribution to cosmic ray time signal on long term scales. Okpala *et al*. (2015) showed that the magnetic field component of solar wind is a dominant factor affecting the variability of monthly mean values of cosmic rays for high latitude stations. They however did not study the amplitude and phase features of such monthly mean variation and their association with heliospheric forcing and geomagnetic activity.

CHAPTER THREE

THEORY, METHOD OF DATA ANALYSIS AND RESULTS

3.1 SOURCE OF DATA

The data used for this project was obtained from Space Physics Interactive Data Resource (SPIDR) (http://spidr.ngdc.noaa.gov/). Table 1 shows the details of four (4) cosmic ray Neutron Monitor (NM) stations used in this work.

Table 1: Characteristics of the four neutron monitor stations used in our study

NEUTRON MONITOR STATION	GEOGRAPHIC LATITUDE (°)	GEOGRAPHIC LONGITUDE (°)	GEOMAGNETIC LATITUDE (°)	GEOMAGNETIC LONGITUDE (°)	CUTOFF RIGIDITY (GV)	ALTITUDE (M)	TYPES OF NEUTRON MONITOR
ROME	41.90	12.52	41.85	93.69	6.32	60	18NM64
OULU	65.05	25.47	61.89	116.86	0.81	0	9NM64
INUVIK	68.35	226.28	70.95	272.35	0.18	21	18NM64
THULE	76.61	291.20	86.43	12.91	0.00	260	18NM64

The neutron monitor (NM) is a ground-based detector designed to measure the number of high-energy charged particles striking the Earthós atmosphere from outer space. Most of the times a neutron monitor records galactic cosmic rays and their variation with the 11-year sunspot cycle and 22-year magnetic cycle. Occasionally the sun emits cosmic rays of sufficient energy and intensity to raise radiation levels on earthós surface to the degree that they are readily detected by neutron monitors. They are termed ground level enhancements (GLE) (Meyer et al., 1956).

Data used in this work comprise of cosmic ray count rate from four (4) Neutron Monitor stations (Rome, Oulu, Inuvik and Thule), solar and geomagnetic activity index. The sunspot number is used here as an index of solar activity. The aa index represents the geomagnetic activity level at an invariant magnetic latitude at about 50 degrees. The daily values are found from an average of the 8 (3 hour interval) values.

3.2 THEORY AND METHOD OF DATA ANALYSIS

In this work the five (5) international quietest days were employed. These days are believed to experience the least geomagnetic disturbance in a month. It is assumed in this work that using these quiet days has the advantage of eliminating transient variations of cosmic rays (Ground Level Enhancement and Forbush Decreases) from the study. The hourly means of the five (5) quietest days were used to obtain the diurnal profile for each month. Thus one-thousand, six hundred and twenty (1,620) quietest days were used to obtain the diurnal profile for 324 months (or 27 years) which were considered in this study. Equation (2) describes the intensity (X) of hourly means of the five (5) quietest days;

$$X_i = \frac{1}{5}\sum_{j=1}^{5} C_{ij} \tag{2}$$

C_{ij} is the raw cosmic ray count rate for a particular hour i, for a given quietest day j.

j = 1 to 5.

The monthly mean count rate, diurnal amplitude, diurnal phase-time and dispersion of the quiet dayôs cosmic ray count rate for the four stations (Table 1) were obtained from the theory of Discrete Fourier Transform (DFT) performed on the complex diurnal data using the MATLAB software. Discrete Fourier Transform (DFT) takes a finite number of samples of a signal and transforms them into a finite number of frequency samples of that signal. DFT applies to signals that exist at a finite number of time points and produces a finite number of frequency points. In this work, the first harmonic from our Discrete Fourier Transform was considered. Cosmic ray intensity (CRI) at the time t_i can be represented by equation (4) being the DFT equation.

$$I_i = f(t) = a_0 + \sum_{n=1}^{24}\left(a_n \cos(nt) + b_n \sin(nt)\right) \qquad (3a)$$

gives

$$I_i = f(t) = a_0 + \sum_{n=1}^{24}\left(r_n \cos(nt) - \phi_n\right) \qquad (3b)$$

where;

$$r_n = \left(a_n{}^2 + b_n{}^2\right)^{1/2} \qquad (3c)$$

$$\phi_n = \tan^{-1}\left(\frac{a_n}{b_n}\right) \qquad (3d)$$

where a_0 is the monthly mean count rate, r_n is the diurnal amplitude and $\dot{\varepsilon}_n$ the phase-time of CR. Equation (4) is the dispersion relation; it is a measure of the fit of equation (3b)

$$d = \sum_{i=1}^{n} d^2 = \sum_{i=1}^{n}[X_i - f(t_i)]^2 = \sum_{i=1}^{n}[X_i - I_i]^2 \qquad (4)$$

where X_i, is the measured data point at time i, n = 24 (hours).

Equation (4) is a measure of quality of fit for equation (3b) and is important for investigating the diurnal deviations of cosmic ray intensity. Figures (4 to 7) illustrate the monthly Sq diurnal variation with the fit of the first harmonic for the four stations.

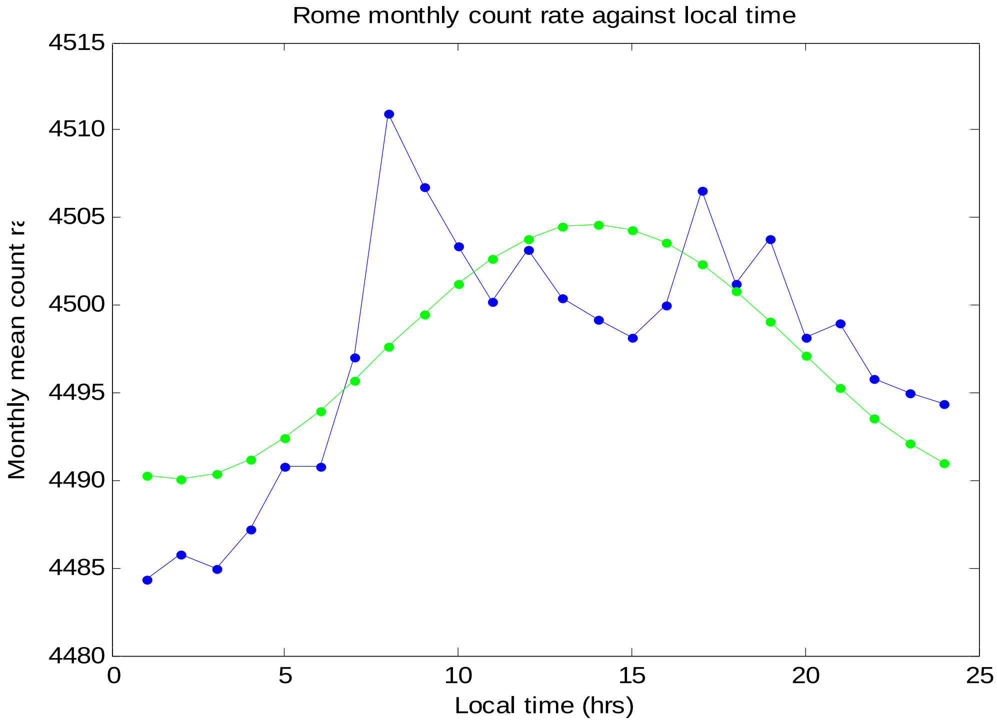

Figure 4: Monthly SQ diurnal variation with the fit of the first harmonic for Rome station.

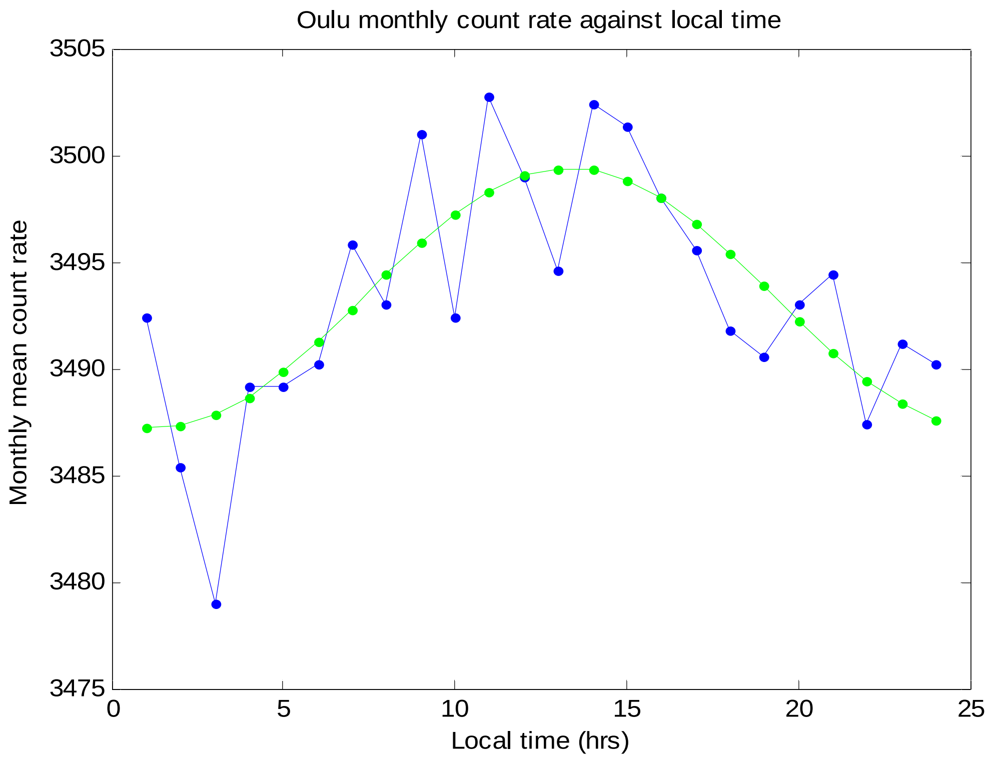

Figure 5: Monthly SQ diurnal variation with the fit of the first harmonic for Oulu station.

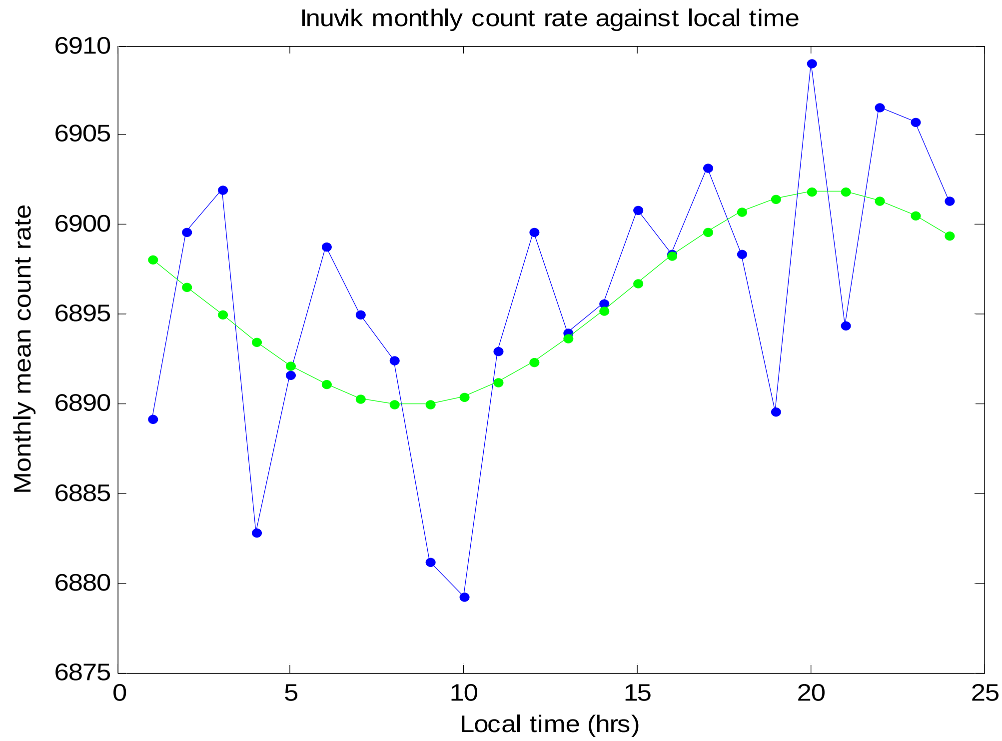

Figure 6: Monthly SQ diurnal variation with the fit of the first harmonic for Inuvik station.

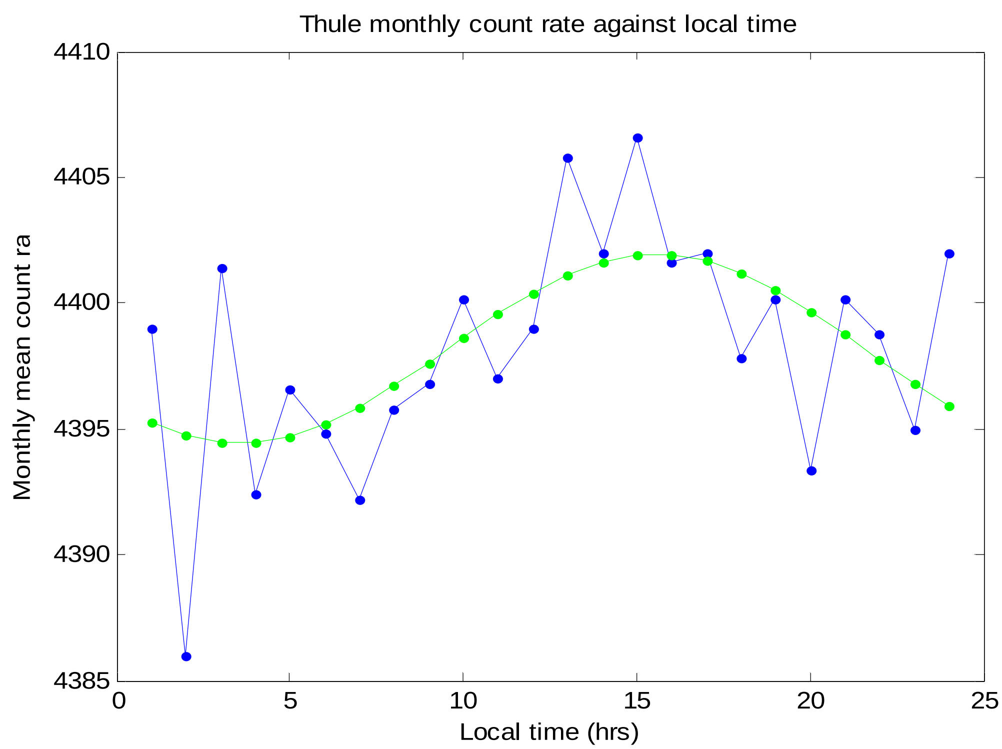

Figure 7: Monthly SQ diurnal variation with the fit of the first harmonic for Thule station.

The count rates for all stations were normalized such that the value of the mean of October 2007 was 100%. This is to reduce the effect of the differences in the instrument from one station to the other. The profile of the monthly mean count rates is shown in Figure (8).

The monthly mean of the daily sunspot number and aa index were obtained; this represents solar activity and geomagnetic activity respectively, their linear correlations with the monthly mean count rate and amplitude were obtained. The formulas for Pearsonĝs linear correlation and partial correlation are given by equations (5) and (6) respectively.

$$r = \frac{N\sum xy - \left(\sum x\right)\left(\sum y\right)}{\sqrt{\left[N\sum x^2 - \left(\sum x\right)^2\right]\left[N\sum y^2 - \left(\sum y\right)^2\right]}} \tag{5}$$

$$r_{xy.z} = \frac{r_{xy} - r_{xz}r_{yz}}{\sqrt{\left(1 - r_{xz}^{\ 2}\right)\left(1 - r_{yz}^{\ 2}\right)}} \tag{6}$$

where x represents dataset $\{x_{1,}$é $, x_n\}$, y represents the second dataset $\{y_{1,}$é $, y_n\}$, z represents the third dataset $\{z_{1,}$é $z_n\}$ and each dataset contain N number of values.

These correlations were obtained at 0.05 significance level. Student T-test was carried out to determine the significance of the correlations. Equation (7) adequately describes the student T-test.

$$T = \frac{\overline{X}_1 - \overline{X}_2}{\sqrt{\frac{S_1^{\ 2}}{n_1} + \frac{S_2^{\ 2}}{n_2}}} \tag{7}$$

$\overline{X}_1$ = Mean of first dataset.

$\overline{X}_2$ = Mean of second dataset.

S_1 = Standard deviation of first dataset.

S_2 = Standard deviation of second dataset.

n_1 = Number of values in the first dataset.

n_2 = Number of values on the second dataset.

3.3 RESULTS

Appendix B shows the results of the Discrete Fourier Transform we performed. %Monthly mean, %diurnal amplitude, diurnal phase-time and dispersion were obtained from the MATLAB script presented in Appendix A. We used values produced from our analysis presented in the Appendices of Tables to make plots that will be discussed.

3.3.1 TIME SERIES PROFILES OF MONTHLY MEAN, AMPLITUDE AND DISPERSION

The time series plots of monthly percentage count rate and amplitude for each station are presented in Figures 8 and 9 respectively. Figure 10 shows the time series plot of the dispersion observed from the transformed data. The dispersion is a measure of how much the fit deviates from the complex wave form. The time series plot of sunspot number has been superimposed on the time series plot of Rome in Figure 8A.

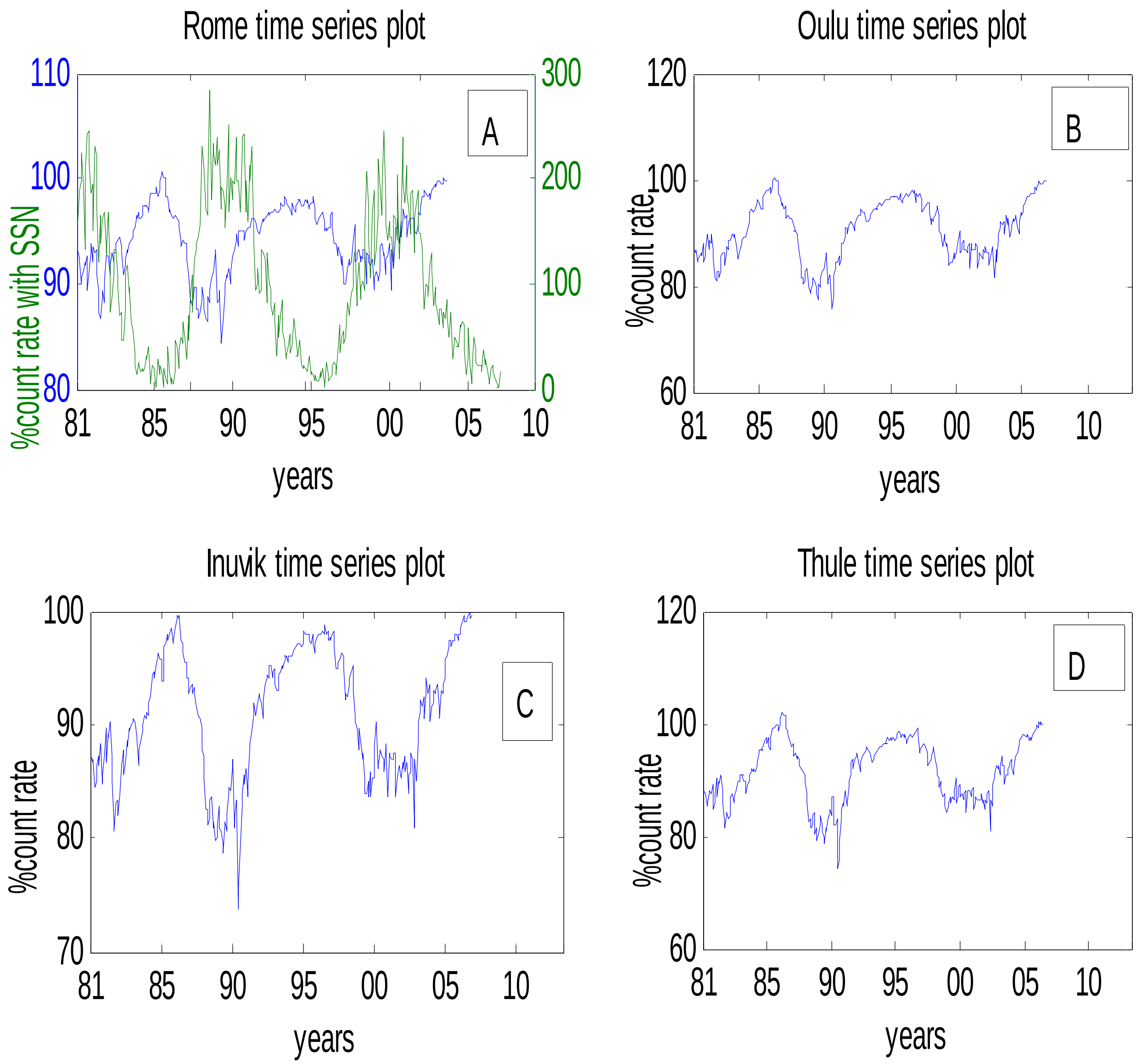

Figure 8: Time series of the monthly mean count rates for the four stations.

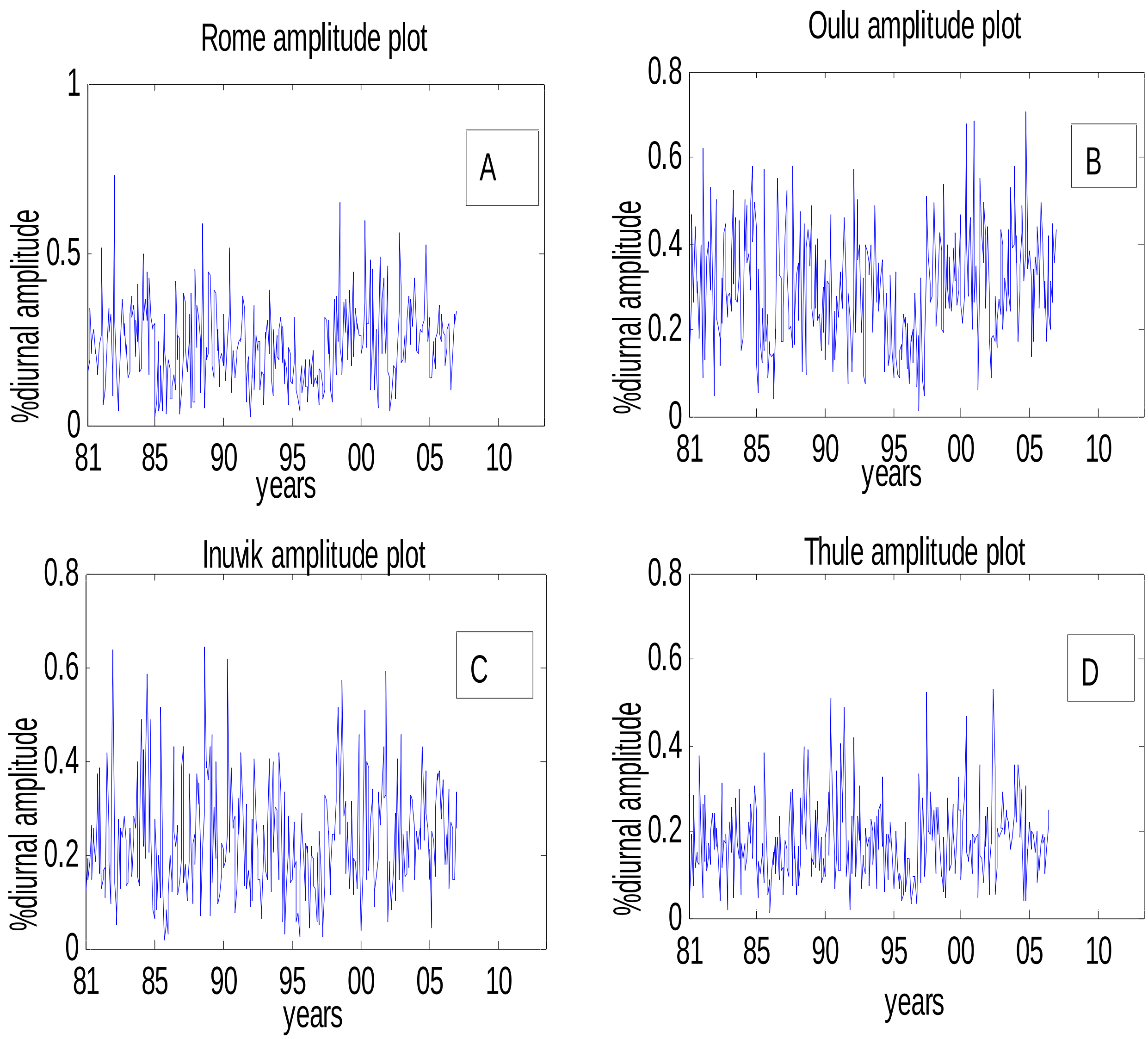

Figure 9: Time series of the monthly diurnal amplitude for the four stations.

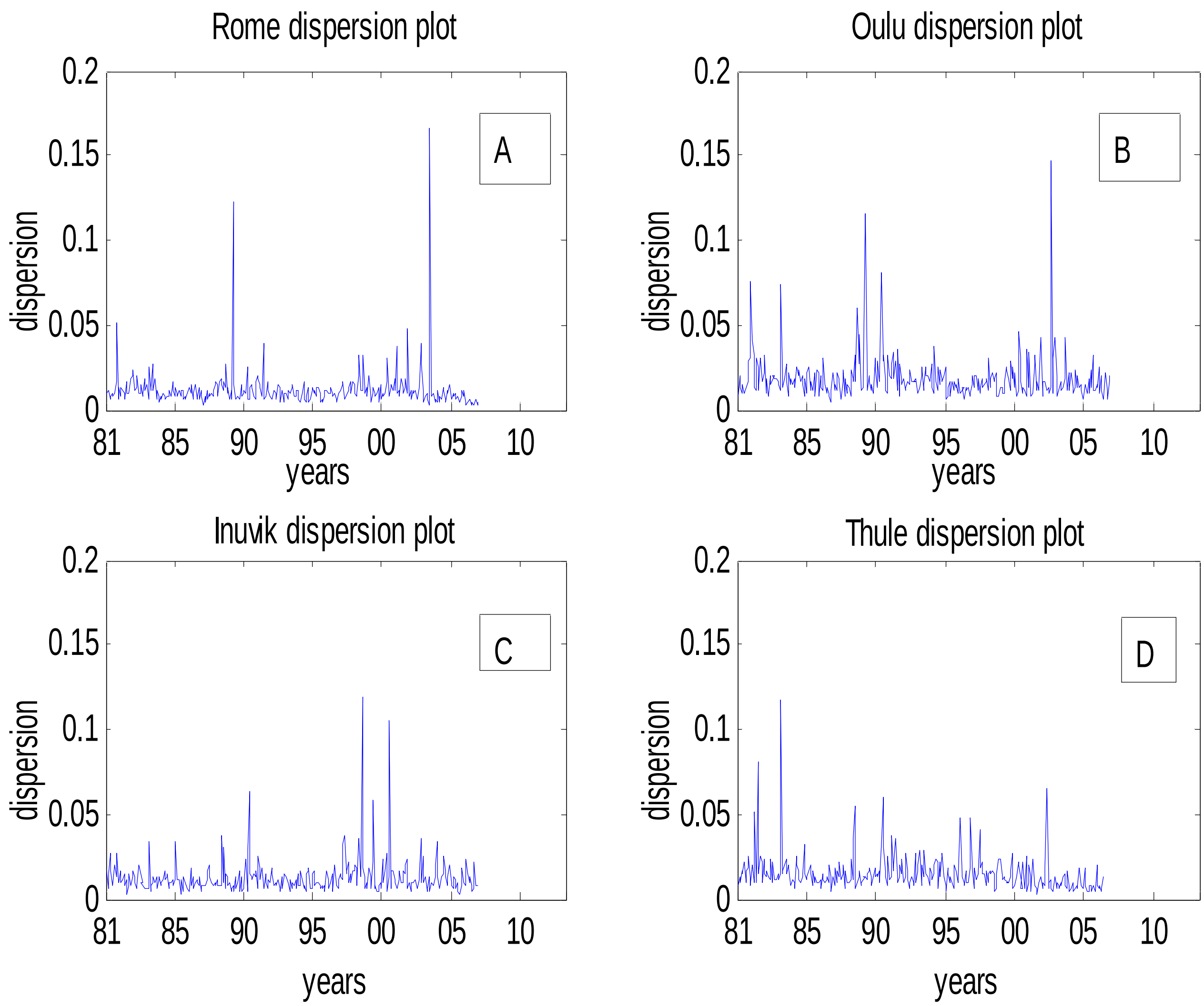

Figure 10: Time series of the dispersion for the four stations.

3.3.2 PHASE-TIME HISTOGRAMS

The frequencies of the phase over the period of study (1981-2007) are shown in Figure 11.

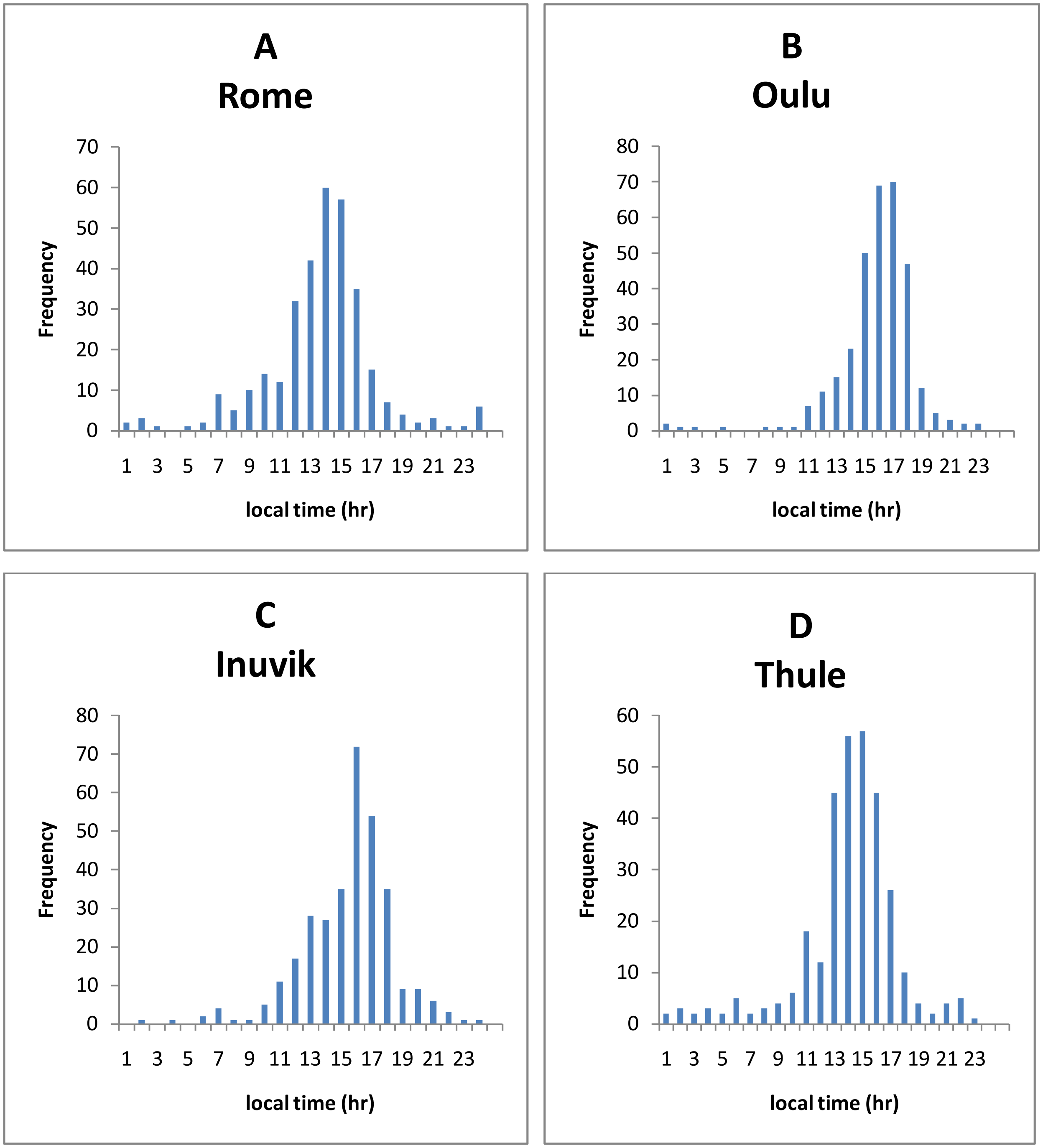

Figure 11: Phase-time histograms for all stations.

For Figures 12 to 15, we define;

Solar minimum 1 = phase hours of (1985, 1986, 1987);

Solar minimum 2 = phase hours of (1995, 1996, 1997);

Solar minimum 3 = phase hours of (2006, 2007);

Solar maximum 1 = phase hours of (1988, 1989, 1990);

Solar maximum 2 = phase hours of (1999, 2000, 2001).

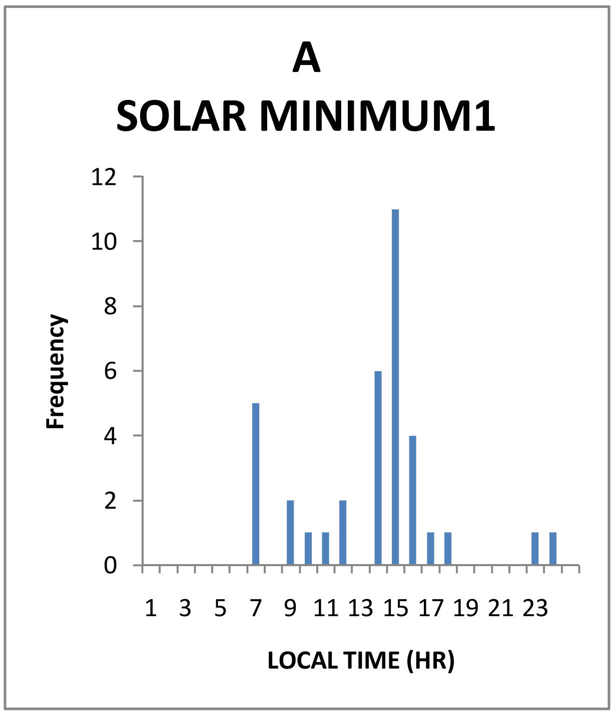

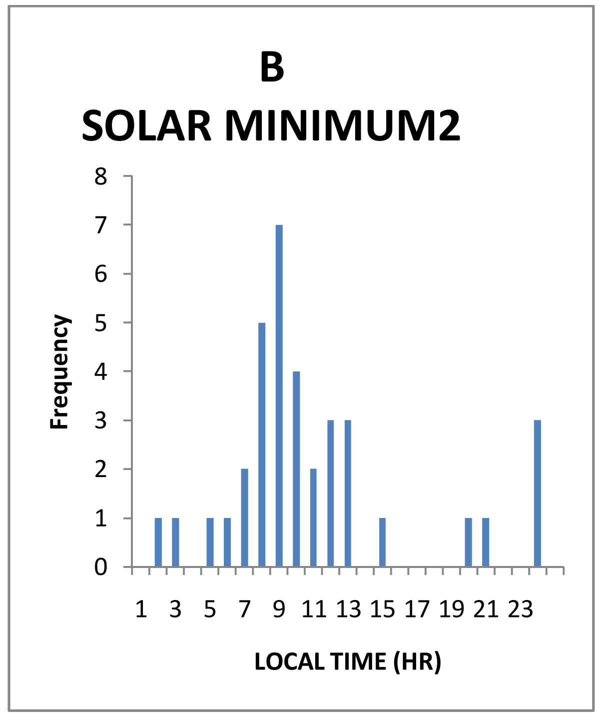

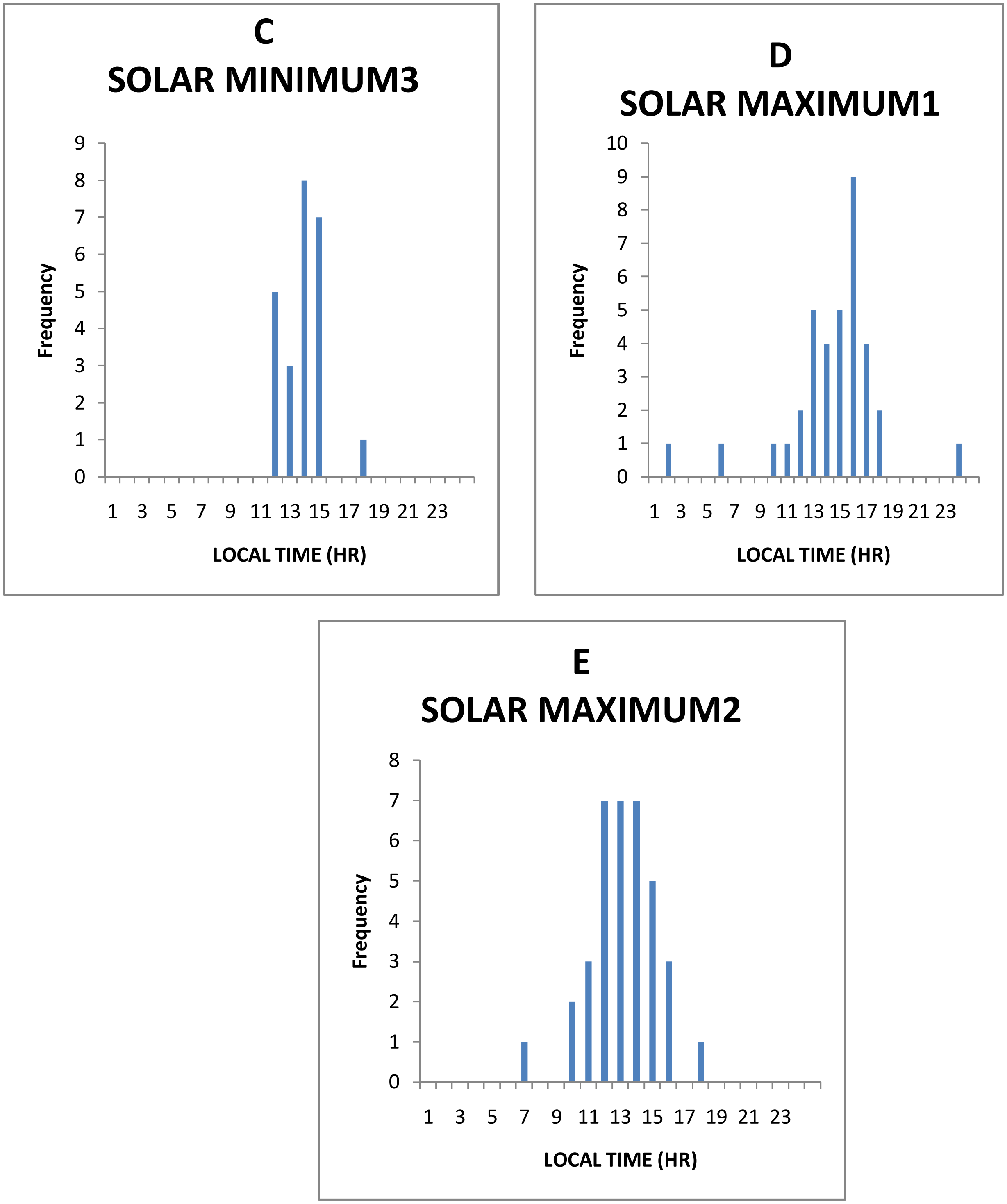

Figure 12: Phase-time histograms for Rome station.

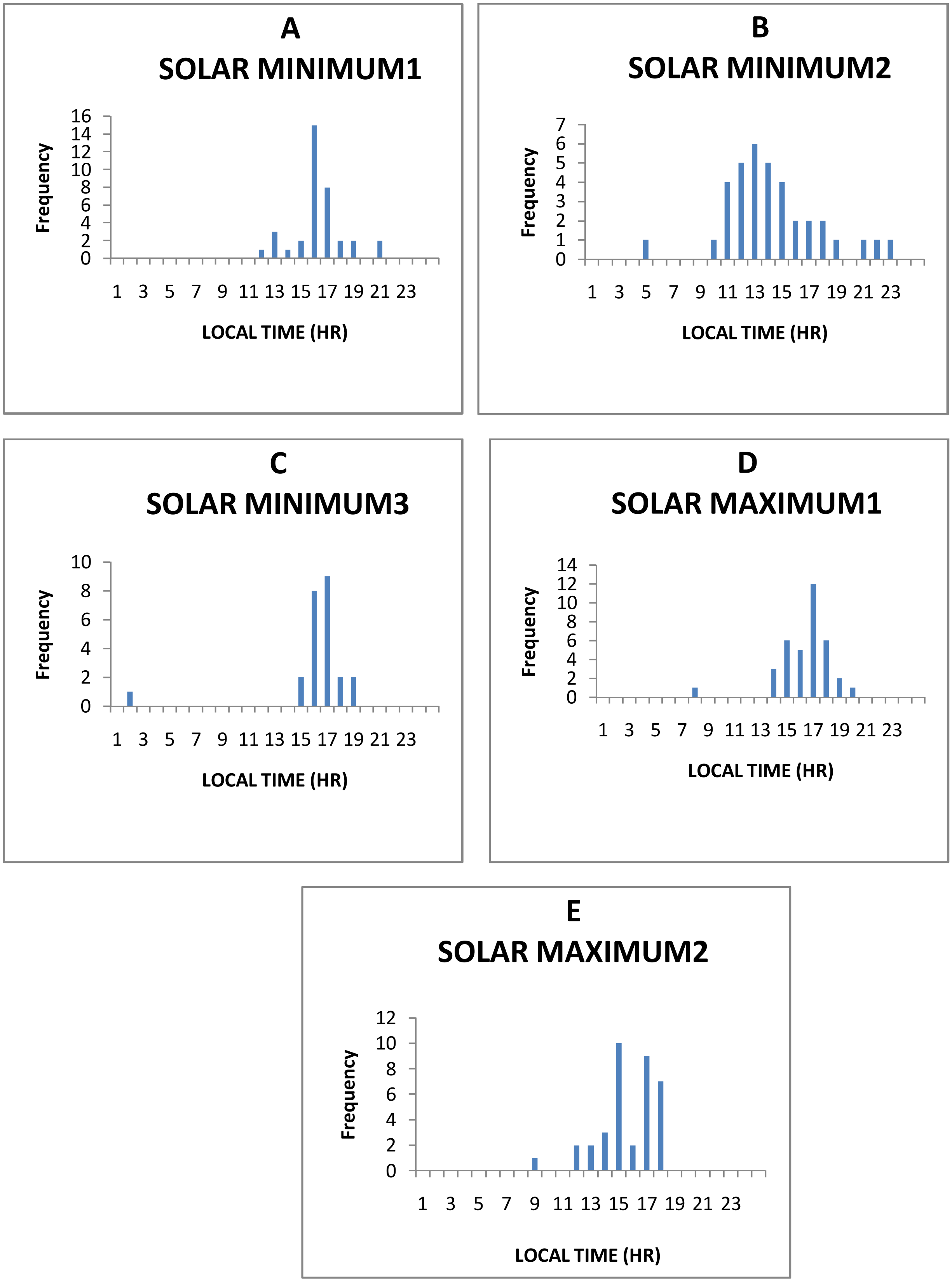

Figure 13: Phase-time histograms for Oulu station.

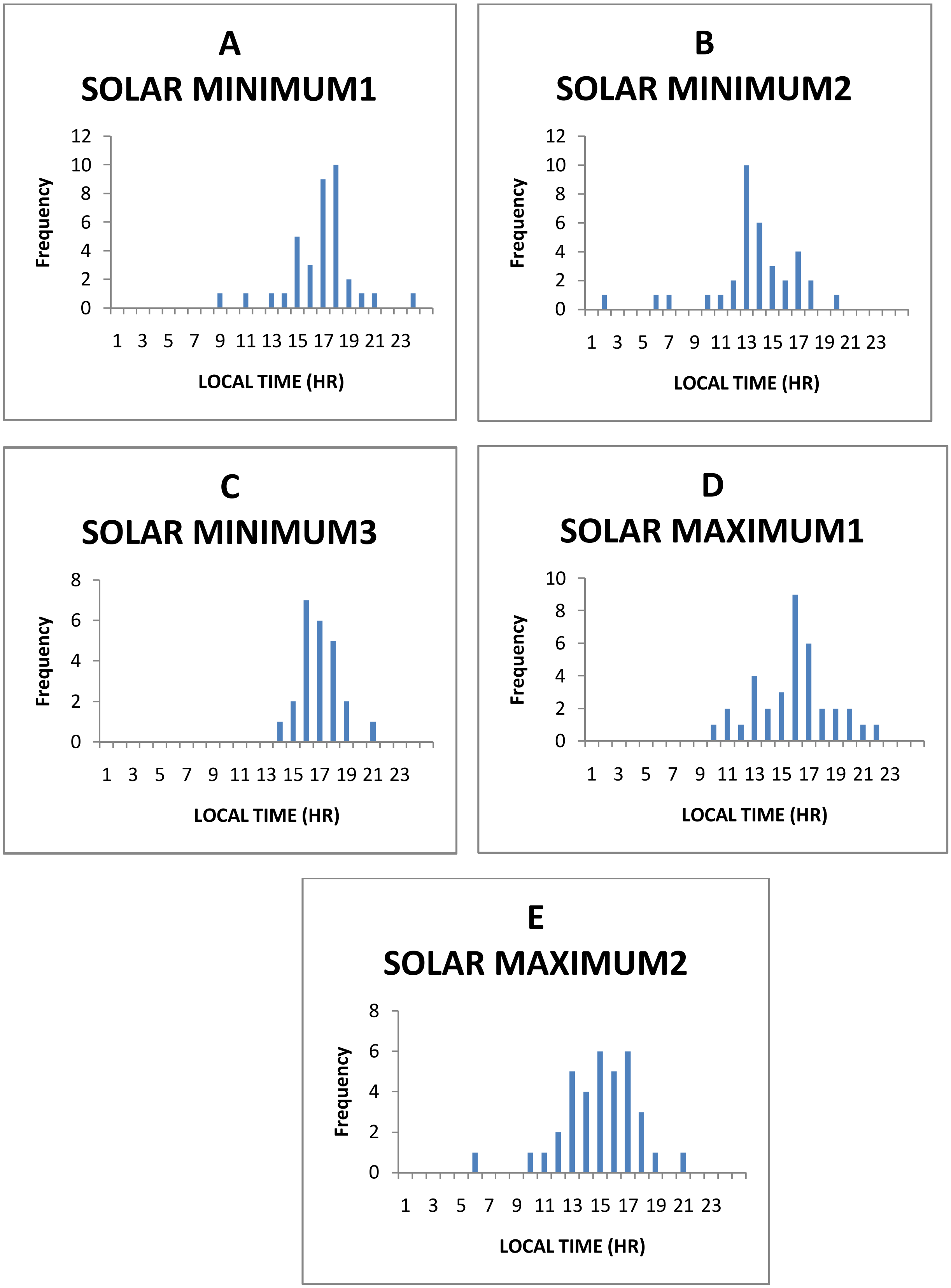

Figure 14: Phase-time histograms for Inuvik station.

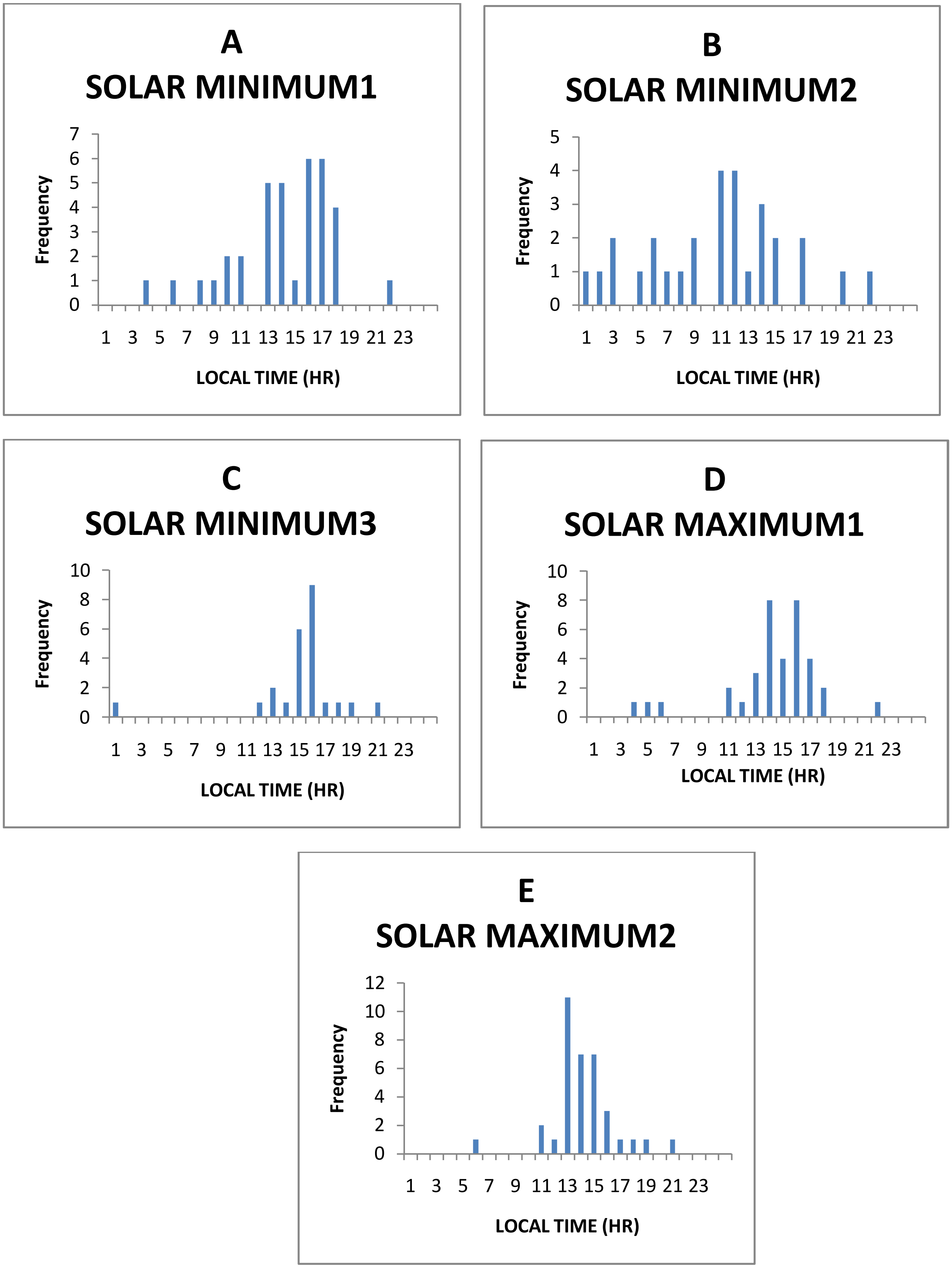

Figure 15: Phase-time histograms for Thule station.

3.3.3 CORRELATION RESULTS

Tables 2, 3 and 4 show the inter-station correlation for mean, amplitude and dispersion respectively.

TABLE 2: Inter-station monthly mean count rates correlations

	THULE	INUVIK	OULU	ROME
THULE	1	0.99	0.97	0.97
INUVIK		1	0.97	0.98
OULU			1	0.96
ROME				1

TABLE 3: Inter-station amplitude correlations.

	THULE	INUVIK	OULU	ROME
THULE	1	0.47	0.49	0.41
INUVIK		1	0.57	0.57
OULU			1	0.7
ROME				1

TABLE 4: Inter-station dispersion correlations

	THULE	INUVIK	OULU	ROME
THULE	1	0.19	0.25	0.12
INUVIK		1	0.3	0.24
OULU			1	0.41
ROME				1

Tables 5 and 6 show the respective mean and amplitude correlation with sunspot number and aurora indices for all stations.

TABLE 5: Geomagnetic activity index (aa) and sunspot number correlation (and partial correlation) with the monthly mean count rates of all four stations.

MEAN	SSN	aa index (SSN removed)
THULE	-0.81	-0.56 (-0.46)
INUVIK	-0.82	-0.58 (-0.50)
OULU	-0.79	-0.57 (-0.46)
ROME	-0.81	-0.56 (-0.45)

TABLE 6: Geomagnetic activity index (aa) and sunspot number correlation (and partial correlation) with the amplitude of all four stations.

AMP	SSN	aa index (SSN removed)
THULE	0.18	0.20 (0.14)
INUVIK	0.14	0.14 (0.10)
OULU	0.06	-0.06 (-0.04)
ROME	0.20	0.17 (0.10)

CHAPTER FOUR

DISCUSSION OF RESULTS

4.1 INTRODUCTION

The quiet time monthly mean count rate of the dataset was obtained from equation (2) alongside amplitude and phase of the diurnal wave of cosmic ray flux received at four neutron monitor stations. The amplitude of the diurnal variation is the maximum displacement obtained after Fourier analysing the discrete dataset while the phase refers to the particular hour of the maximum displacement. The interest here is to study the trends and features of the cosmic ray solar quiet dayõs variations and their associations with solar and geomagnetic activities. To achieve this, cosmic ray count rate data from four cosmic ray neutron monitor stations have been subjected to harmonic analysis and the time series of the monthly mean, amplitude and dispersion have been obtained. In addition, the phase distributions of the stations diurnal wave have been obtained and are discussed in this chapter.

4.2 TIME SERIES OF MONTHLY MEAN AND AMPLITUDE OF DIURNAL WAVE OF COSMIC RAYS

Figure 8 shows the monthly mean count rate (in percentage normalized to the value of October 2007) of the four stations. The figure shows the classical inverse association of cosmic ray count rates with solar activity as can be seen in Figure 8A; low count rate during solar maxima (1988-1990, 1999-2001) and higher count rates during solar minima (1985-1987, 1995-1997, 2006-2007); this agrees with (Balasubrahmanyan, 1968). The sharp peak followed by broad peak after eleven (11) year interval (1985-1995) is a validation of the method used and is consistent with the twenty-two (22) year solar activity cycles as reported in earlier works (e.g. Hester *et al*., 2002, Okpala and Okeke, 2011).

Notice that Figure 8 has strikingly similar temporal variations for all stations with respective mid-latitude and aurora region stations (Rome and Inuvik) showing more dramatic spatial variation during the solar maxima periods (8A and C). The troughs (solar maxima) are usually associated with multiple peaks. The peaks of aurora station (Inuvik) and mid-latitude station (Rome) during solar maxima are more intense than the peaks at Thule and Oulu. The behaviour of peaks noticed during solar maxima periods at the mid-latitude station (Rome) could be attributed to ring current observed in the region as stations in this region are used with low latitude stations to measure ring current. The injection of current in the aurora region as a result of the openness of the geomagnetic field in that area contributes to cosmic ray variability in the region as can be seen in Inuvik station especially during solar maximum periods. The quiet time monthly mean values of the normalized CR flux for the four stations generally show similar trends which suggest a common source of modulation.

The amplitude plots Fig. 9 showed that the maximum displacements seem to follow an 11-year periodicity. This was seen to be inversely related to the time series plots of the stations, with higher amplitudes at the solar maxima.

Tables 2 and 3 show the inter-station correlation for the monthly mean count rate and amplitude. Very good association was seen for the monthly mean count rate of the four stations, ranging from 0.96 - 0.99. We observed moderate correlations ranging from 0.47-0.70 for the inter-station amplitude correlation. These correlations were significant at 0.05 significant levels. Tables 5 and 6 show the respective monthly mean count rate and amplitude correlation with sunspot number and geomagnetic activity index (aa) for all stations. The geomagnetic activity index correlated moderately with monthly mean count rate in the inverse direction for all stations; removing the effect of solar activity (SSN) on their association showed a decrease in the value of their correlation but it wasnꞌt sufficient to infer that the original association was spurious. The aa-index correlated weakly with the amplitude. The sunspot number correlated strongly in the inverse direction with the monthly mean count rate of the various stations. This suggests that sunspot number (solar activity) has a significant contribution to the variability of cosmic ray count rate. The sunspot number correlated weakly with the amplitude.

4.3 DISPERSION PROFILE

The dispersion is a measure of how the NM count rate deviated from the ideal variability. Figure 11 shows the time series plots of the dispersion for the four stations. It is evident that there is similarity between the profiles of Oulu and Rome stations; showing sharp dispersions close to 1989 and 2003. Inuvik and Thule showed lesser dispersion. Solar maxima periods are more dispersed. Inter-station dispersion correlation was poor. Rome and Oulu showed greater dispersion correlation (with 0.41) as can be seen in Table 4.

4.4 PHASE-TIME VARIABILITY OF COSMIC RAY DIURNAL WAVE

Histograms showing the frequency of phase-time (local time) for each station used are presented in Figure 12. Rome had many phase time between 12th – 16th hours with the most occurrence on the 14th hour. Oulu had many phase time between 15th – 18th hours with the most occurrences on the 16th and 17th hours. Inuvik had many phase time between 13th – 18th hours with the most occurrences on the 16th and 17th hours. Thule had many phase time between 13th – 16th hours with the most occurrences on the 14th and 15th hours.

To study the solar activity dependent features of the phase-time, we grouped the years used in the study into solar maxima and minima periods. The frequencies of the phase-time for the various stations are displayed in Figures 12 to 15. Summary of the profiles of the histograms in Figures 12 to 15 is presented in Table 7.

Table 7: Stations phase-time frequency records around solar minimum and maximum periods.

ROME		OULU		INUVIK		THULE	
Solar cycle	**MOST OCCURING PHASE HOUR(S)**	**Solar cycle**	**MOST OCCURIN G PHASE HOUR(S)**	**Solar cycle**	**MOST OCCURIN G PHASE HOUR(S)**	**Solar cycle**	**MOST OCCURIN G PHASE HOUR(S)**
Solar minimum 1	15TH HR	**Solar minimum 1**	16TH HR	**Solar minimum1**	17TH & 18TH HRS	**Solar minimum 1**	16TH & 17TH HRS
Solar minimum 2	9TH HR	**Solar minimum 2**	12TH,13TH & 14TH HRS	**Solar minimum2**	13TH & 14TH HRS	**Solar minimum 2**	11TH & 12TH HRS
Solar minimum 3	14TH & 15TH HRS	**Solar minimum 3**	16TH & 17TH HRS	**Solar minimum3**	16TH & 17TH HRS	**Solar minimum 3**	15TH & 16TH HRS
Solar maximum 1	16TH HOUR	**Solar maximum 1**	17TH HR	**Solar maximum 1**	16TH & 17TH HRS	**Solar maximum 1**	14TH & 16TH HRS
Solar maximum 2	12TH,13TH & 14TH HRS	**Solar maximum 2**	15TH & 17TH HRS	**Solar maximum 2**	13TH, 15TH & 17TH HRS	**Solar maximum 2**	13TH,14TH & 15TH HRS

From the table above, comparing solar minima 1, 2 and 3; it is can be observed that solar minima 1 and 3 have very close phase time for all the stations. Solar minimum 2 phase time is earlier when compared to solar minima (1 and 3). The difference noticed could be because of the sharp and broad peak nature of these cycles caused primarily by pole reversal of the sun. For solar maximum 1 and solar maximum 2; we observed that the phase time is quite close with solar maximum 2 coming slightly earlier than solar maximum 1. This shows that the phase time follows a twenty-two (22) year variability pattern thereby giving credence to the solar modulation of cosmic rays count rates.

CHAPTER FIVE

CONCLUSIONS AND RECOMMENDATION

5.1 CONCLUSIONS

In this work, we have studied the features and properties of cosmic ray (CR) diurnal wave on quiet days to identify their dependence on solar and geomagnetic activities. Four stations (one mid-latitude station, one high latitude station with two aurora region stations) have been employed for this work. The data used covers two and half (2½) solar cycles. The following conclusions were made from the results obtained in this study:

i. The cosmic ray monthly mean count rates in all four stations are highly correlated showing similar temporal variation with marked spatial variation during solar maximum.

ii. Sharp and broad peaks in the solar quiet time monthly mean count rate seen over 22 year period can be associated with the sunõs polar magnetic field reversal.

iii. The spatial variation in solar quiet monthly mean cosmic ray count rates tend to be controlled by aurora and ring current geomagnetic activity rather than rigidity of the cosmic rays.

iv. Quiet time monthly mean cosmic ray count rate are more associated with solar activity than with geomagnetic activity at both mid and high latitudes. The variability of the amplitude was not associated with either geomagnetic or solar activity in all stations.

v. There was more dispersion during solar maximum period. The diurnal waves of the higher latitude stations are less dispersive especially during solar active periods.

vi. The phase variations tend to follow the twenty-two (22) year solar magnetic activity cycle. It is characterized by a 2-6 hour change between periods of peak and minimum solar activity.

5.2 RECOMMENDATION

Considering that cosmic rays are modulated by interaction with geophysical space and heliosphere as they approach the earth, it is necessary to understand specific heliophysical processes which may contribute to this modulation. Specifically, it may be necessary to understand quantitatively the amount of the modulation of the cosmic ray that can be attributed to heliophysical forcing, and what amount can be associated with geophysical forcing through spectral analysis.

There is equally a need to further this work to the southern hemisphere for verification of the results obtained here.

REFERENCES

Agarwal, R. and Mishra, R.K. (2008). Modulation of cosmic rays at different cutoff rigidity. Brazilian Journal of Physics, 38, 108-116.

Ananth, A.G., Vankatesan, D. and Pillai, S. (1993). long term changes in cosmic ray diurnal anisotropy. Solar Physics, 143, 187-196.

Balasubrahmanyan, V. K. (1968). Solar activity and the 11-year modulation of cosmic rays. Solar Physics, 7(1), 39-45.

Bazilevskaya, B. A., Krainev, M. B., Makhmutov, V. S., Stozhkov, Y. I., Svirzhevskaya, A. K. and Svirzhevsky, N. S. (1995). The relationship between the galactic cosmic ray intensity and the sunspot distribution. Advance Space Research, 16(9), 221-225.

Belov, A.V., Gushchina, R.T and Yanke, V.G (1999). The spectrum of cosmic rays variations during 19-22 solar cycles. Proceedings of the 26th international cosmic conference, 7, 175-178.

Chillingarian, A. and Mailyan, R. (2009). Investigation of diurnal variation of cosmic ray flux in the Beginning of 24th Solar Activity Cycle. proceedings of the 31st ICRC, LODZ, 1-4.

Firoz, K. A. (2008). On cosmic ray diurnal variations: Disturbed and Quiet days. WDSâ08 proceedings of contributed papers, part II, 183-188.

Helen, M. and Evangelos, P. (2012). Long term cosmic ray variability and the CME-index. Advances in Astronomy, 2012, 1-8.

Hester, J., David, B., George, B., Ronald, G., Bradford, S., Howard, V. and Gary, W. (2002). 21st Century Astronomy. New York NY: W.W. Norton & company Inc. publishers. 345-350.

Kane, R.P. (2009). High amplitude anisotropic events (HAE) in cosmic ray diurnal variation during solar cycle 23. Indian Journal of Radio and Space Physics, 38, 189-196.

Kudela, K., Firoz, K.A., Langer, R.D. and Kollir, V. (2008). On diurnal variation of cosmic rays: statistical study of neutron monitor data including Lomnicky stit. Proceedings of the 21st European cosmic ray conference, 2008, 374-378.

Kudela, K. and Sabbah, I. (2016). Quasi-periodic variations of low energy cosmic rays. Science China Technological Sciences, 59(4), 547-557.

Kumar S., Shrivastava, S.K., Dubey, S.K., Richaria, M.K. and Gulati, U. (1998). Effect of solar poloidal magnetic field reversal on diurnal anisotropy of cosmic ray intensity on quiet days. Indian Journal of Radio and Space Physics, 27, 236-240.

Meyer, P., Parker, E. N., and Simpson, J. A. (1956). Solar cosmic rays of February, 1956 and their propagation through interplanetary space. Physical Review 104 (3), 768-783.

Okpala, K. C. (2015). Galactic cosmic ray variability at two neutron monitors: relation to Kp index. Journal of Astrophysics, 2015, 1-5.

Okpala, K.C. and Okeke, F.N. (2011). Investigation of diurnal and seasonal galactic cosmic ray variation on quite days in two mid latitude stations. Astroparticle Physics, 34, 878ï 885.

Okpala, K.C., Okeke, F.N. and Ugwoke, A.I., (2015). Cosmic ray modulation in high and middle latitudes during solar cycles 22 and 23. Canadian Journal of Physics, 93(1), 100-104.

Pomerantz, M.A. and Duggal, S.P. (1971). The cosmic ray solar diurnal anisotropy. Space Science Review, 12, 75-130.

Sabbah, I. (2007). Twenty-seven day variation of galactic cosmic rays, Solar Physics. 245, 207-217.

Sabbah, I. and Kudela, K. (2011). Third harmonic of the 27 periodicity of galactic cosmic rays: coupling with interplanetary parameters. Journal of Geophysical Research: Space Physics, 116(A4), 2156-2202.

Shea, M. A. and Smart, D. F. (1990). The influence of the changing geomagnetic field on cosmic ray measurements. Journal of Geomagnetism and Geoelectricity, 42, 1107-1121.

Shea, M. A. and Smart, D. F. (2004). Preliminary study of cosmic rays, geomagnetic field changes and possible climate changes. Advances in Space Research, 34, 420-425.

Singer, S.F. (1952). Cosmic rays and the sunǿs magnetic field: Diurnal variation of cosmic rays and the sunǿs magnetic field. Nature, 170; 63-64.

Singh, Y.P. and Badruddin (2015). Solar rotational oscillation and its harmonics in the solar wind, geomagnetic and cosmic ray particles during the last two solar minima. Astrophysics and Space Science, 359, 60.

Stormer. C. (1955). The polar aurora. Oxford University Press.

Svensmark, H. (2007). Cosmoclimatology: a new theory emerge. Astronomy and Geophysics, 48(1); 18-24.

Tiwari, R. K., Achyut, P., Pankaj, K. S. and Sushil, K. S. (2011). Relationship of cosmic rays with solar and geomagnetic activity. Indian Journal of Scientific Research, 2(4), 15-19.

Usoskin, I. G. and Kalevi, M. (2001). Heliospheric modulation of cosmic rays and solar activity during the maunder minimum. Journal of Geophysical research, 106(A8), 16039 ï 16046.

APPENDIX A: MATLAB script for DFT

```
clear all
load Sqdays_cosmicTHULE.dat;          % Loads the Sq hourly values for 1 year data (1981)for
a THULE
month=Sqdays_cosmicTHULE (:,2);          %% Specify each column
year=Sqdays_cosmicTHULE(:,1);
day=Sqdays_cosmicTHULE(:,3);

% data1=Sqdays_cosmicTHULE(1440*10+1:1440*11,5);

data1=Sqdays_cosmicTHULE(:,5);
%data3=data2-data1;
% plot (data1)       % Plot data to confirm it looks like what you expect

data1(data1==0)=NaN;

b=reshape(data1,24,1585);
for i=1:317;
   for j=1:24;
   y(j,i) = nanmean(b(j,i*5-4:5*i)');
   end
end


y=y(:,299);
% b=reshape(data1,24,60); y=b(:,6);
%%
ni=24;
nb=24;
nf=1;
ts=1:24;
low=2000;
high=8000;
fet=5.0;
dod=1;
delta=0.1;
Opt.FirstRun=true;

%%
```

```
[amp_none,phi_none,yr_none]=HANTS(ni,nb,nf,y,ts,'none',low,high,fet,dod,delta);

%%
[amp_Lo,phi_Lo,yr_Lo]=HANTS(ni,nb,nf,y,ts,'Lo',low,high,fet,dod,delta);

%%
[amp_Hi,phi_Hi,yr_Hi]=HANTS(ni,nb,nf,y,ts,'Hi',low,high,fet,dod,delta);


%% plotting
plot(y,'b.-');
hold on;
% plot(yr_Lo,'r.-');
% plot(yr_Hi,'k.-');
plot(yr_none,'g.-');
% legend('Original Data','HANTS - Lo','HANTS - Hi','HANTS - none');
% title('Testing HANTS 2009 Algorithm')
```

APPENDIX B: COMPUTED RESULTS FROM DFT

ROME CR COUNT RATE RESULTS FROM DFT

Years	Months	%Monthly mean CR	%Diurnal Amplitude	Diurnal phase-time	Dispersion
81	1	93.118	0.151	13	0.0096
81	2	92.239	0.194	12	0.0109
81	3	91.99	0.337	13	0.0117
81	4	89.959	0.205	13	0.0064
81	5	90.447	0.244	12	0.0072
81	6	91.131	0.28	13	0.0092
81	7	92.041	0.209	12	0.0084
81	8	91.718	0.22	12	0.009
81	9	92.483	0.16	9	0.017
81	10	89.261	0.145	15	0.0515
81	11	91.209	0.237	13	0.0061
81	12	92.842	0.261	15	0.0132
82	1	93.817	0.522	11	0.0081
82	2	92.12	0.199	11	0.0135
82	3	93.48	0.06	10	0.0106
82	4	92.887	0.103	13	0.0088
82	5	93.357	0.224	14	0.0054
82	6	90.944	0.236	15	0.0166
82	7	89.497	0.342	14	0.0096
82	8	87.282	0.273	13	0.0098
82	9	86.586	0.324	14	0.0104
82	10	88.8	0.138	24	0.0174
82	11	89.367	0.085	11	0.0203
82	12	88.289	0.729	11	0.0242
83	1	90.247	0.301	14	0.0111
83	2	92.747	0.142	18	0.0117
83	3	92.701	0.043	20	0.0133
83	4	92.605	0.074	15	0.0195
83	5	90.733	0.213	13	0.0096
83	6	91.662	0.243	14	0.0103
83	7	92.89	0.369	14	0.0154
83	8	92.131	0.262	16	0.0072
83	9	92.99	0.294	15	0.0094
83	10	92.954	0.208	12	0.0177
83	11	93.833	0.237	12	0.011
83	12	94.138	0.14	12	0.0153
84	1	94.07	0.157	17	0.0057

84	2	94.304	0.327	15	0.025
84	3	93.391	0.376	12	0.0118
84	4	93.059	0.316	11	0.0129
84	5	90.982	0.349	13	0.0263
84	6	91.684	0.198	14	0.0115
84	7	92.309	0.305	13	0.0186
84	8	93.087	0.247	12	0.0062
84	9	92.998	0.408	11	0.0112
84	10	93.771	0.154	14	0.0078
84	11	93.728	0.161	14	0.0046
84	12	94.106	0.203	12	0.0079
85	1	94.51	0.499	12	0.0058
85	2	94.97	0.305	13	0.0088
85	3	95.304	0.368	13	0.0077
85	4	96.446	0.301	14	0.0056
85	5	96.329	0.443	13	0.0082
85	6	96.722	0.149	14	0.0086
85	7	96.236	0.427	14	0.0085
85	8	96.205	0.314	13	0.0112
85	9	96.481	0.275	12	0.0073
85	10	97.245	0.291	14	0.0159
85	11	97.566	0.3	13	0.0106
85	12	97.367	0.02	9	0.0075
86	1	97.454	0.064	6	0.0135
86	2	97.082	0.243	10	0.0094
86	3	96.842	0.042	10	0.008
86	4	98.629	0.077	15	0.0109
86	5	98.447	0.172	14	0.0082
86	6	98.463	0.036	10	0.0105
86	7	98.264	0.322	13	0.0117
86	8	98.436	0.222	13	0.0056
86	9	98.699	0.162	6	0.0086
86	10	99.278	0.034	14	0.0069
86	11	98.289	0.188	6	0.0101
86	12	98.987	0.162	6	0.0137
87	1	99.897	0.073	13	0.0123
87	2	100.456	0.078	8	0.0093
87	3	100.528	0.113	23	0.0155
87	4	99.955	0.142	6	0.0065
87	5	99.948	0.1	22	0.0087
87	6	98.159	0.423	12	0.0155
87	7	98.323	0.188	13	0.0063
87	8	98.292	0.259	14	0.0073

87	9	96.743	0.253	13	0.0131
87	10	97.142	0.033	16	0.0056
87	11	96.533	0.094	8	0.0108
87	12	96.572	0.21	14	0.0078
88	1	96.203	0.387	12	0.0031
88	2	96.147	0.355	11	0.0071
88	3	96.349	0.228	12	0.0052
88	4	96.086	0.152	14	0.011
88	5	95.777	0.247	15	0.0062
88	6	95.19	0.326	15	0.0088
88	7	94.223	0.046	9	0.0074
88	8	93.598	0.388	13	0.0091
88	9	93.992	0.069	13	0.0071
88	10	93.891	0.066	14	0.0119
88	11	93.74	0.452	16	0.0156
88	12	93.892	0.228	11	0.0163
89	1	92.243	0.35	13	0.0151
89	2	90.893	0.316	12	0.0081
89	3	88.275	0.239	16	0.0165
89	4	88.564	0.092	0	0.0182
89	5	87.823	0.42	14	0.0142
89	6	87.888	0.587	17	0.0118
89	7	89.523	0.051	23	0.0169
89	8	89.69	0.222	9	0.0122
89	9	87.542	0.188	12	0.0275
89	10	87.61	0.209	15	0.0104
89	11	86.624	0.449	15	0.0129
89	12	87.317	0.442	11	0.0068
90	1	88.44	0.236	13	0.0115
90	2	89.532	0.173	14	0.0064
90	3	88.393	0.135	4	0.1219
90	4	87.474	0.393	14	0.0153
90	5	86.757	0.383	15	0.0054
90	6	86.384	0.214	15	0.0061
90	7	88.681	0.281	10	0.0086
90	8	88.245	0.112	13	0.0078
90	9	89.298	0.191	14	0.0057
90	10	90.488	0.204	13	0.014
90	11	91.23	0.172	15	0.0071
90	12	91.162	0.324	11	0.0103
91	1	92.882	0.131	12	0.0105
91	2	93.123	0.127	12	0.0103
91	3	88.168	0.245	13	0.0245

91	4	88.553	0.327	14	0.0065
91	5	89.357	0.515	17	0.0069
91	6	84.882	0.224	14	0.0123
91	7	84.38	0.091	19	0.0148
91	8	86.336	0.213	13	0.0135
91	9	89.169	0.145	14	0.0081
91	10	89.836	0.135	12	0.0058
91	11	90.841	0.198	14	0.0157
91	12	90.524	0.216	10	0.02
92	1	91.373	0.244	12	0.0186
92	2	89.876	0.25	11	0.0155
92	3	91.012	0.244	12	0.0132
92	4	92.727	0.331	11	0.0084
92	5	92.65	0.374	12	0.0386
92	6	93.197	0.339	11	0.0059
92	7	94.227	0.062	15	0.0076
92	8	94.644	0.131	18	0.0078
92	9	93.528	0.196	13	0.0165
92	10	94.981	0.153	14	0.0118
92	11	94.956	0.02	12	0.0074
92	12	95.353	0.148	11	0.0086
93	1	94.975	0.136	14	0.0054
93	2	95.069	0.352	11	0.0116
93	3	94.192	0.106	16	0.0109
93	4	94.97	0.261	11	0.0094
93	5	95.084	0.218	11	0.0069
93	6	95.286	0.245	12	0.0146
93	7	95.341	0.246	12	0.0131
93	8	95.231	0.104	15	0.0051
93	9	96.067	0.157	15	0.0117
93	10	96.065	0.142	22	0.0119
93	11	96.082	0.055	24	0.0044
93	12	95.933	0.272	13	0.0091
94	1	95.815	0.249	9	0.01
94	2	95.111	0.307	12	0.0066
94	3	94.737	0.209	8	0.0112
94	4	94.842	0.39	9	0.0111
94	5	95.552	0.267	11	0.0089
94	6	95.664	0.136	15	0.0128
94	7	96.174	0.08	6	0.0145
94	8	95.849	0.279	9	0.0082
94	9	96.312	0.164	9	0.0079
94	10	96.483	0.261	11	0.0117

94	11	96.534	0.198	10	0.0119
94	12	96.719	0.192	11	0.0061
95	1	96.527	0.277	8	0.0061
95	2	96.714	0.312	6	0.0036
95	3	96.709	0.18	7	0.0094
95	4	96.715	0.291	8	0.0161
95	5	97	0.12	9	0.0055
95	6	96.954	0.186	6	0.0035
95	7	96.79	0.168	23	0.0078
95	8	96.887	0.059	11	0.0127
95	9	96.907	0.227	4	0.0051
95	10	97.153	0.212	8	0.0061
95	11	97.554	0.129	8	0.0108
95	12	97.4	0.12	6	0.0125
96	1	97.423	0.183	22	0.0087
96	2	98.274	0.312	19	0.0108
96	3	98.05	0.133	22	0.0077
96	4	97.625	0.1	6	0.0122
96	5	97.31	0.071	1	0.013
96	6	97.32	0.036	1	0.0089
96	7	97.223	0.122	10	0.0044
96	8	96.579	0.17	7	0.0055
96	9	97.614	0.094	11	0.0049
96	10	96.975	0.124	11	0.0082
96	11	96.735	0.193	8	0.0117
96	12	97.356	0.107	9	0.0109
97	1	97.588	0.111	11	0.0119
97	2	97.858	0.066	20	0.0092
97	3	97.897	0.188	10	0.0091
97	4	97.412	0.116	8	0.0126
97	5	97.242	0.161	6	0.0087
97	6	97.411	0.218	9	0.0082
97	7	97.424	0.112	7	0.0103
97	8	97.823	0.138	7	0.0054
97	9	97.632	0.123	10	0.0038
97	10	97.999	0.146	8	0.0093
97	11	97.153	0.054	4	0.0088
97	12	97.434	0.167	13	0.0118
98	1	97.576	0.151	10	0.0114
98	2	97.646	0.115	9	0.0155
98	3	98.219	0.075	15	0.0165
98	4	97.186	0.099	16	0.0066
98	5	96.17	0.313	13	0.0093

98	6	95.7	0.305	12	0.0111
98	7	96.181	0.211	10	0.0105
98	8	96.138	0.303	14	0.0124
98	9	96.281	0.115	11	0.0171
98	10	96.518	0.1	16	0.0087
98	11	96.803	0.066	12	0.0161
98	12	95.938	0.369	11	0.0148
99	1	94.883	0.357	11	0.009
99	2	95.437	0.142	10	0.0086
99	3	95.071	0.374	10	0.009
99	4	95.194	0.246	10	0.0193
99	5	95.437	0.647	10	0.0319
99	6	96.432	0.227	10	0.0114
99	7	96.901	0.177	14	0.0114
99	8	95.36	0.142	5	0.033
99	9	93.831	0.357	13	0.0136
99	10	93.89	0.272	12	0.0103
99	11	93.843	0.37	9	0.0127
99	12	92.576	0.258	9	0.0079
0	1	93.653	0.186	12	0.0202
0	2	92.965	0.397	12	0.0083
0	3	91.715	0.175	13	0.0047
0	4	92.478	0.26	11	0.009
0	5	90.667	0.446	10	0.0128
0	6	89.817	0.203	17	0.0095
0	7	90.037	0.338	12	0.0082
0	8	91.468	0.277	15	0.01
0	9	91.486	0.295	14	0.0138
0	10	92.363	0.263	9	0.0043
0	11	91.704	0.263	10	0.0151
0	12	91.764	0.262	13	0.0055
1	1	91.97	0.21	12	0.0096
1	2	94.005	0.234	12	0.0083
1	3	95.685	0.354	12	0.0102
1	4	92.117	0.596	12	0.016
1	5	92.18	0.222	15	0.0309
1	6	93.005	0.299	12	0.0094
1	7	93.291	0.296	11	0.0076
1	8	92.02	0.478	14	0.0133
1	9	92.549	0.104	14	0.0143
1	10	92.388	0.249	12	0.0119
1	11	93.243	0.458	13	0.018
1	12	93.342	0.099	11	0.0117

2	1	90.034	0.275	13	0.0367
2	2	93.031	0.16	11	0.0091
2	3	92.493	0.052	13	0.0113
2	4	91.987	0.202	13	0.0077
2	5	91.679	0.489	15	0.0176
2	6	92.319	0.212	13	0.0134
2	7	92.236	0.366	13	0.0101
2	8	89.365	0.425	13	0.0135
2	9	90.66	0.334	14	0.0188
2	10	91.023	0.206	11	0.0093
2	11	90.673	0.461	8	0.0479
2	12	90.19	0.159	10	0.0073
3	1	91.269	0.138	13	0.0105
3	2	93.403	0.043	17	0.0057
3	3	93.75	0.082	1	0.0117
3	4	92.694	0.163	15	0.0087
3	5	92.989	0.175	10	0.0116
3	6	90.785	0.163	14	0.0121
3	7	92.382	0.076	17	0.0065
3	8	92.727	0.219	13	0.0129
3	9	93.847	0.33	11	0.0131
3	10	93.553	0.564	13	0.0386
3	11	89.457	0.407	13	0.0262
3	12	93.282	0.179	15	0.0115
4	1	91.317	0.193	8	0.0044
4	2	94.489	0.263	14	0.007
4	3	95.292	0.181	11	0.0099
4	4	95.221	0.281	14	0.0065
4	5	96.325	0.309	13	0.0029
4	6	93.696	0.373	20	0.1653
4	7	95.944	0.237	12	0.007
4	8	94.506	0.366	14	0.0082
4	9	96.196	0.287	11	0.0102
4	10	96.94	0.297	13	0.0037
4	11	96.216	0.425	13	0.0063
4	12	96.378	0.282	14	0.0045
5	1	94.461	0.216	14	0.0106
5	2	96.023	0.208	12	0.0052
5	3	95.823	0.214	12	0.0073
5	4	96.187	0.275	12	0.0058
5	5	96.32	0.274	15	0.0122
5	6	96.114	0.29	12	0.011
5	7	96.32	0.306	12	0.0063

5	8	95.133	0.305	12	0.005
5	9	94.585	0.523	13	0.0117
5	10	95.534	0.249	13	0.0098
5	11	96.64	0.24	12	0.014
5	12	96.617	0.312	13	0.0055
6	1	97.188	0.136	12	0.0054
6	2	98.402	0.141	11	0.0096
6	3	98.4	0.243	11	0.0076
6	4	98.761	0.211	16	0.0097
6	5	98.69	0.166	12	0.0064
6	6	98.666	0.248	13	0.0073
6	7	98.159	0.27	13	0.0086
6	8	98.643	0.349	13	0.0042
6	9	98.092	0.268	13	0.0075
6	10	98.74	0.247	13	0.0121
6	11	98.821	0.327	11	0.0072
6	12	99.014	0.269	12	0.0107
7	1	99.341	0.26	13	0.0042
7	2	99.035	0.169	12	0.0024
7	3	99.678	0.228	14	0.0047
7	4	99.855	0.28	10	0.0068
7	5	99.848	0.295	12	0.0053
7	6	99.543	0.111	13	0.0027
7	7	99.497	0.103	13	0.0051
7	8	99.508	0.211	13	0.0021
7	9	99.916	0.212	13	0.0027
7	10	100	0.32	13	0.0062
7	11	99.756	0.294	10	0.003
7	12	99.845	0.329	12	0.0046

OULU CR COUNT RATE RESULTS FROM DFT

Years	Months	%Monthly mean CR	%Diurnal amplitude	Diurnal phase-time	Dispersion
81	1	87	0.151	12	0.0074
81	2	86.4	0.261	12	0.0204
81	3	86.7	0.466	14	0.0127

81	4	84.3	0.265	14	0.0101
81	5	85	0.283	14	0.0149
81	6	85.7	0.436	16	0.0102
81	7	86.3	0.283	14	0.0123
81	8	85.7	0.309	14	0.0126
81	9	87.7	0.194	13	0.0163
81	10	84.3	0.18	1	0.0281
81	11	85.4	0.395	15	0.0306
81	12	87	0.09	12	0.0751
82	1	89.7	0.621	13	0.0402
82	2	86.8	0.245	14	0.0323
82	3	88.5	0.131	13	0.0128
82	4	88.1	0.369	15	0.011
82	5	89.7	0.404	14	0.0302
82	6	86.9	0.383	16	0.0245
82	7	84.8	0.288	14	0.0113
82	8	81.2	0.529	15	0.0311
82	9	80.7	0.334	15	0.0163
82	10	82.4	0.049	17	0.0161
82	11	82.9	0.266	16	0.0225
82	12	81.4	0.503	13	0.0321
83	1	82.4	0.229	15	0.0088
83	2	85.7	0.205	12	0.0186
83	3	86.1	0.179	14	0.0071
83	4	86.4	0.119	11	0.02
83	5	84	0.32	13	0.0149
83	6	85.9	0.212	16	0.0186
83	7	87.4	0.426	15	0.0201
83	8	86.8	0.448	16	0.0201
83	9	88.6	0.29	16	0.0184
83	10	88.7	0.226	10	0.0174
83	11	89.7	0.279	13	0.0173
83	12	89.6	0.286	18	0.0152
84	1	89.1	0.241	15	0.0113
84	2	89.5	0.38	14	0.0736
84	3	87.9	0.523	13	0.0226
84	4	87.8	0.305	13	0.0125
84	5	85.2	0.463	15	0.0183
84	6	86.6	0.273	16	0.0269
84	7	87	0.263	14	0.0162
84	8	88.1	0.329	14	0.007
84	9	88.5	0.456	14	0.0226
84	10	88.9	0.17	16	0.0145

84	11	88.9	0.151	16	0.018
84	12	89	0.179	13	0.0156
85	1	91.2	0.504	14	0.0185
85	2	92.1	0.382	12	0.0122
85	3	92.3	0.487	15	0.0251
85	4	93.7	0.354	15	0.0256
85	5	94	0.375	15	0.0206
85	6	94.3	0.293	14	0.023
85	7	94	0.496	15	0.0172
85	8	93.6	0.582	13	0.0201
85	9	94.6	0.403	14	0.0156
85	10	95.3	0.495	17	0.0078
85	11	96	0.441	14	0.0184
85	12	95.4	0.124	11	0.0087
86	1	95.6	0.052	18	0.0215
86	2	94.3	0.341	13	0.0254
86	3	94.2	0.17	11	0.0119
86	4	97	0.123	15	0.0158
86	5	97.3	0.251	14	0.0114
86	6	97.5	0.149	14	0.011
86	7	97.5	0.569	15	0.0221
86	8	97.7	0.169	14	0.0072
86	9	98.1	0.236	9	0.0231
86	10	98.6	0.091	13	0.0219
86	11	97.2	0.175	11	0.0077
86	12	98.6	0.142	12	0.0208
87	1	99.8	0.135	13	0.0135
87	2	100.3	0.144	11	0.0108
87	3	100.1	0.04	19	0.03
87	4	99.7	0.2	14	0.0155
87	5	99.8	0.179	15	0.0098
87	6	97.4	0.552	14	0.0129
87	7	97	0.369	13	0.0094
87	8	96.5	0.324	13	0.0085
87	9	95.2	0.318	14	0.0038
87	10	95.4	0.173	15	0.0117
87	11	94.7	0.173	13	0.022
87	12	95.1	0.247	16	0.011
88	1	92.5	0.416	14	0.0155
88	2	92.8	0.524	13	0.0105
88	3	93.3	0.343	14	0.0216
88	4	92.6	0.234	12	0.018
88	5	92.7	0.201	15	0.0167

88	6	92.5	0.205	15	0.0064
88	7	90.7	0.158	12	0.0165
88	8	90.4	0.581	15	0.0236
88	9	90.2	0.168	15	0.0072
88	10	90.3	0.229	14	0.0181
88	11	89.5	0.324	17	0.0093
88	12	88.9	0.352	12	0.0146
89	1	86	0.22	14	0.0133
89	2	84	0.473	12	0.0083
89	3	81.2	0.446	15	0.0242
89	4	81.6	0.104	14	0.0175
89	5	80.3	0.438	14	0.017
89	6	80.8	0.445	18	0.0327
89	7	82.5	0.097	16	0.0159
89	8	83.4	0.391	14	0.06
89	9	79.7	0.429	12	0.0276
89	10	80	0.388	16	0.045
89	11	78.4	0.35	15	0.012
89	12	79.4	0.49	12	0.0113
90	1	80.3	0.25	14	0.0131
90	2	81.7	0.21	13	0.0179
90	3	80.6	0.398	5	0.1164
90	4	79.8	0.252	15	0.0209
90	5	78.5	0.41	15	0.0109
90	6	77.4	0.22	15	0.0201
90	7	80.3	0.233	12	0.016
90	8	79.9	0.148	14	0.0105
90	9	81.3	0.194	14	0.0148
90	10	82.7	0.3	15	0.0097
90	11	83.5	0.19	16	0.0301
90	12	83.4	0.364	13	0.0239
91	1	85.3	0.131	14	0.0131
91	2	86.1	0.314	14	0.0284
91	3	80.4	0.308	14	0.0166
91	4	80.7	0.163	15	0.0159
91	5	81.9	0.469	18	0.0805
91	6	76.4	0.365	15	0.0284
91	7	75.8	0.105	13	0.0329
91	8	78	0.241	15	0.0189
91	9	81.9	0.132	15	0.0108
91	10	83	0.216	14	0.0093
91	11	84.3	0.277	14	0.0322
91	12	84.5	0.226	11	0.0196

92	1	85.3	0.333	12	0.0184
92	2	83.7	0.31	15	0.0278
92	3	84.9	0.252	15	0.0339
92	4	87.7	0.313	12	0.0176
92	5	87.8	0.462	13	0.0295
92	6	89.1	0.309	13	0.0106
92	7	90.6	0.301	12	0.0363
92	8	91	0.073	19	0.0082
92	9	89.6	0.285	12	0.0265
92	10	91.3	0.226	16	0.0174
92	11	91.3	0.119	9	0.0153
92	12	91.9	0.102	10	0.0177
93	1	91.7	0.247	15	0.0118
93	2	91.6	0.571	14	0.0123
93	3	90.1	0.194	13	0.0164
93	4	91.5	0.5	12	0.0162
93	5	92.4	0.361	13	0.015
93	6	92.9	0.398	14	0.0228
93	7	93.1	0.391	15	0.0172
93	8	93.2	0.19	13	0.018
93	9	94.3	0.322	13	0.0166
93	10	94.2	0.095	20	0.0166
93	11	93.9	0.071	11	0.0181
93	12	93.7	0.397	15	0.0091
94	1	93.9	0.385	12	0.0098
94	2	92.2	0.354	13	0.0123
94	3	92.1	0.326	9	0.0192
94	4	92.2	0.396	12	0.0247
94	5	92.5	0.365	12	0.0107
94	6	93.3	0.193	15	0.0142
94	7	93.8	0.202	10	0.0255
94	8	93.8	0.491	12	0.0192
94	9	94.6	0.264	12	0.0195
94	10	94.9	0.281	14	0.016
94	11	94.3	0.351	13	0.0171
94	12	94.2	0.243	13	0.0273
95	1	95.1	0.319	11	0.0135
95	2	95.2	0.362	9	0.0088
95	3	95.3	0.341	9	0.0371
95	4	95.2	0.228	12	0.0162
95	5	95.6	0.101	12	0.0105
95	6	95.6	0.286	10	0.0251
95	7	95.9	0.135	19	0.0152

95	8	96	0.116	12	0.0242
95	9	96.1	0.144	8	0.0177
95	10	96.2	0.325	13	0.017
95	11	96.1	0.154	11	0.0199
95	12	95.9	0.09	11	0.0252
96	1	96.7	0.142	2	0.0063
96	2	97.4	0.33	20	0.0077
96	3	96.8	0.135	7	0.0134
96	4	96.9	0.097	9	0.0159
96	5	96.9	0.087	10	0.0079
96	6	97	0.154	12	0.0169
96	7	96.9	0.168	13	0.0105
96	8	96.2	0.131	8	0.0166
96	9	97.2	0.232	14	0.013
96	10	96.1	0.21	15	0.014
96	11	95.5	0.229	11	0.0091
96	12	96.1	0.108	16	0.0174
97	1	97	0.216	14	0.0098
97	2	97.2	0.072	14	0.0109
97	3	97.4	0.187	11	0.0128
97	4	97.3	0.174	10	0.0134
97	5	97	0.199	10	0.0069
97	6	97.4	0.126	12	0.0123
97	7	97.1	0.281	11	0.0118
97	8	97.8	0.146	10	0.0127
97	9	97.6	0.067	10	0.0081
97	10	98.1	0.188	17	0.0099
97	11	95.6	0.008	20	0.0153
97	12	97.2	0.292	15	0.0199
98	1	96.5	0.319	10	0.0126
98	2	96.5	0.082	11	0.0207
98	3	97.2	0.043	23	0.0193
98	4	95.9	0.16	12	0.0121
98	5	93.9	0.334	15	0.0185
98	6	93.9	0.51	16	0.0088
98	7	94.7	0.37	12	0.0138
98	8	94.7	0.308	14	0.0187
98	9	94.8	0.261	12	0.0133
98	10	95.4	0.275	17	0.0154
98	11	95.4	0.288	12	0.0173
98	12	94.1	0.498	13	0.0179
99	1	91.7	0.307	13	0.0116
99	2	92.4	0.206	13	0.0299

99	3	92	0.279	11	0.0135
99	4	92.9	0.297	12	0.0179
99	5	93.3	0.424	11	0.0209
99	6	94.2	0.383	13	0.0158
99	7	95.2	0.203	14	0.0175
99	8	93	0.191	7	0.0209
99	9	90.5	0.538	14	0.0086
99	10	89.8	0.247	12	0.0081
99	11	89.5	0.396	12	0.0077
99	12	87.5	0.301	10	0.0122
0	1	89.5	0.248	14	0.0133
0	2	88.5	0.368	13	0.0094
0	3	87.1	0.24	12	0.0098
0	4	87.7	0.315	15	0.0172
0	5	85.8	0.391	11	0.0249
0	6	84.1	0.309	15	0.0232
0	7	84.2	0.423	14	0.0189
0	8	84.7	0.257	12	0.0109
0	9	84.5	0.288	15	0.028
0	10	86.2	0.334	10	0.0176
0	11	85.1	0.465	12	0.0256
0	12	86	0.258	15	0.0127
1	1	86.1	0.216	15	0.0219
1	2	88.4	0.223	14	0.0079
1	3	90.3	0.275	15	0.012
1	4	86.2	0.678	14	0.046
1	5	86.8	0.396	16	0.03
1	6	87.8	0.276	14	0.0164
1	7	88.3	0.37	12	0.009
1	8	86.9	0.461	15	0.013
1	9	87	0.202	15	0.012
1	10	86.2	0.236	12	0.0084
1	11	87.1	0.687	15	0.0365
1	12	87.7	0.26	16	0.0128
2	1	83.5	0.344	16	0.0345
2	2	87.8	0.179	12	0.0086
2	3	86.8	0.063	14	0.0074
2	4	86.9	0.348	13	0.0099
2	5	86.8	0.552	17	0.0271
2	6	87.9	0.415	13	0.0327
2	7	87.3	0.356	13	0.0119
2	8	83.5	0.497	14	0.0158
2	9	85.1	0.42	15	0.0119

2	10	86	0.246	12	0.0147
2	11	85.5	0.441	9	0.0431
2	12	84.8	0.283	12	0.0085
3	1	86.5	0.177	16	0.0163
3	2	86.3	0.085	16	0.0164
3	3	87.1	0.181	13	0.0157
3	4	86.1	0.185	14	0.0105
3	5	86.3	0.171	14	0.0131
3	6	83.9	0.28	16	0.0096
3	7	85.6	0.16	16	0.013
3	8	85.4	0.222	22	0.1467
3	9	87.4	0.27	17	0.0089
3	10	87	0.232	15	0.0303
3	11	81.2	0.431	15	0.0434
3	12	86.5	0.396	15	0.0194
4	1	84.5	0.197	8	0.0076
4	2	88.4	0.322	15	0.0176
4	3	90	0.278	13	0.016
4	4	90.7	0.242	14	0.016
4	5	91.8	0.431	15	0.0121
4	6	91.2	0.281	14	0.0139
4	7	91.8	0.245	15	0.0185
4	8	89.8	0.533	16	0.0431
4	9	91.9	0.391	14	0.0133
4	10	93.5	0.399	13	0.0111
4	11	91.7	0.577	14	0.0214
4	12	92.6	0.356	17	0.0109
5	1	89.3	0.417	14	0.0212
5	2	91.1	0.17	12	0.0137
5	3	91.5	0.293	13	0.0097
5	4	92.7	0.347	15	0.013
5	5	92.1	0.425	16	0.0242
5	6	92.6	0.491	13	0.0138
5	7	93.1	0.315	13	0.0206
5	8	91	0.372	14	0.0131
5	9	89.7	0.704	15	0.0152
5	10	92.3	0.428	16	0.0112
5	11	93.7	0.34	14	0.0059
5	12	93.4	0.382	14	0.0057
6	1	93.6	0.319	13	0.0146
6	2	95.1	0.134	13	0.0156
6	3	95.8	0.342	14	0.0099
6	4	96.5	0.173	17	0.0187

6	5	NaN	NaN	NaN	NaN
6	6	96.9	0.371	14	0.0096
6	7	96.5	0.326	14	0.0236
6	8	96.9	0.442	14	0.0136
6	9	96.6	0.363	14	0.0317
6	10	97.4	0.247	14	0.0118
6	11	97.1	0.498	13	0.012
6	12	97.5	0.399	14	0.0147
7	1	98.5	0.383	16	0.0135
7	2	98.2	0.251	14	0.0244
7	3	98.7	0.309	15	0.0104
7	4	99.4	0.173	13	0.0205
7	5	99.7	0.417	15	0.0114
7	6	99.1	0.234	14	0.0063
7	7	99.2	0.2	14	0.0221
7	8	99	0.312	14	0.0214
7	9	99.6	0.263	14	0.0109
7	10	100	0.448	16	0.0061
7	11	99.9	0.351	14	0.0169
7	12	100	0.431	14	0.0203

INUVIK CR COUNT RATE RESULTS FROM DFT

Years	Months	%Monthly mean CR	%Diurnal amplitude	Diurnal phase-time	Dispersion
81	1	87.1	0.117	24	0.0164
81	2	86.7	0.191	1	0.006
81	3	86.9	0.145	1	0.0149
81	4	84.5	0.184	1	0.0266
81	5	85	0.264	24	0.0172
81	6	86.5	0.148	2	0.0073
81	7	87.3	0.255	1	0.0086
81	8	86.5	0.227	24	0.0195
81	9	88.4	0.181	2	0.0129
81	10	84.7	0.299	20	0.0277
81	11	85.6	0.368	0	0.0093

81	12	87.3	0.16	4	0.0089
82	1	89.6	0.385	1	0.0166
82	2	86.7	0.125	22	0.0094
82	3	89	0.143	20	0.0109
82	4	88.8	0.167	23	0.0153
82	5	90.3	0.174	2	0.007
82	6	87.3	0.105	20	0.012
82	7	84.9	0.417	2	0.0033
82	8	81.5	0.256	3	0.007
82	9	80.7	0.181	21	0.0144
82	10	83	0.094	15	0.008
82	11	83.4	0.154	19	0.0126
82	12	81.9	0.636	3	0.0157
83	1	83.7	0.212	2	0.0134
83	2	86.5	0.141	18	0.0088
83	3	86.5	0.076	22	0.0056
83	4	87.7	0.049	22	0.0075
83	5	85.5	0.276	20	0.0201
83	6	86.7	0.123	1	0.0083
83	7	88.6	0.257	1	0.0094
83	8	88	0.238	2	0.0101
83	9	89.6	0.237	2	0.0071
83	10	89.4	0.278	1	0.0062
83	11	89.9	0.231	3	0.0054
83	12	90.1	0.13	21	0.0064
84	1	90.6	0.139	22	0.0057
84	2	90.2	0.159	8	0.0334
84	3	88.9	0.252	3	0.0047
84	4	88.7	0.179	1	0.0082
84	5	86.4	0.151	3	0.0091
84	6	87.7	0.238	2	0.0137
84	7	88.5	0.282	1	0.0087
84	8	89.5	0.257	2	0.0122
84	9	90	0.396	1	0.0064
84	10	90.8	0.15	7	0.012
84	11	90.4	0.134	1	0.0135
84	12	91	0.249	24	0.0076
85	1	90.9	0.489	3	0.0104
85	2	91.9	0.217	23	0.011
85	3	92.5	0.422	3	0.016
85	4	94	0.19	23	0.0111
85	5	94.4	0.355	2	0.0131
85	6	NaN	NaN	NaN	NaN

85	7	94.5	0.582	3	0.0141
85	8	94.2	0.332	3	0.0055
85	9	95.2	0.206	1	0.0099
85	10	95.9	0.485	4	0.0091
85	11	96.2	0.226	2	0.0113
85	12	95.6	0.083	19	0.0075
86	1	95.6	0.062	24	0.0115
86	2	93.8	0.271	3	0.0335
86	3	93.9	0.181	23	0.0116
86	4	96.8	0.081	22	0.0116
86	5	97.2	0.195	3	0.0119
86	6	97.9	0.109	22	0.003
86	7	97.5	0.51	3	0.011
86	8	97.9	0.246	3	0.0048
86	9	97.9	0.149	2	0.0132
86	10	98.5	0.019	24	0.0092
86	11	97.2	0.048	5	0.0091
86	12	97.5	0.079	2	0.0054
87	1	98.4	0.028	3	0.006
87	2	99.3	0.115	0	0.0035
87	3	99.5	0.194	17	0.0179
87	4	99.3	0.138	2	0.0072
87	5	99.5	0.122	4	0.013
87	6	97.5	0.426	2	0.0059
87	7	97	0.25	2	0.0094
87	8	96.3	0.217	3	0.012
87	9	95.4	0.262	2	0.0099
87	10	95.5	0.116	2	0.0081
87	11	94.1	0.137	9	0.0138
87	12	94.1	0.191	6	0.0048
88	1	92.7	0.381	2	0.0085
88	2	93.2	0.427	2	0.0083
88	3	93.6	0.139	24	0.0074
88	4	92.6	0.18	1	0.0077
88	5	93.2	0.101	3	0.0118
88	6	92.6	0.119	1	0.0166
88	7	91.5	0.185	0	0.0198
88	8	90.8	0.371	1	0.0124
88	9	90.9	0.216	24	0.0087
88	10	90.6	0.096	23	0.0102
88	11	89.7	0.224	7	0.008
88	12	87.7	0.243	1	0.0089
89	1	87.1	0.176	5	0.0074

89	2	85.3	0.374	2	0.0105
89	3	82.6	0.304	21	0.0084
89	4	82.5	0.351	0	0.0083
89	5	81.2	0.212	21	0.0086
89	6	81.7	0.068	6	0.037
89	7	83.4	0.208	18	0.0095
89	8	83.6	0.29	4	0.0298
89	9	81	0.641	20	0.0062
89	10	81.5	0.384	2	0.0148
89	11	79.7	0.396	4	0.0134
89	12	80.1	0.359	1	0.0086
90	1	81.2	0.432	2	0.0087
90	2	82.7	0.068	1	0.0051
90	3	80.9	0.452	21	0.0057
90	4	80.5	0.14	20	0.0081
90	5	79.6	0.301	3	0.0044
90	6	78.6	0.189	22	0.0125
90	7	81.3	0.396	24	0.0055
90	8	80.7	0.156	22	0.0101
90	9	82.3	0.096	22	0.016
90	10	83.9	0.113	1	0.0049
90	11	84.5	0.157	5	0.0128
90	12	84.3	0.225	2	0.0035
91	1	86.4	0.211	2	0.0068
91	2	86.9	0.171	23	0.0076
91	3	80.9	0.183	21	0.0227
91	4	81.6	0.24	2	0.0039
91	5	83.4	0.616	6	0.0289
91	6	73.8	0.298	22	0.0636
91	7	75.7	0.205	22	0.0156
91	8	79.2	0.385	22	0.0136
91	9	82.8	0.257	2	0.0114
91	10	84	0.265	3	0.0142
91	11	85.6	0.28	20	0.0128
91	12	84.8	0.075	0	0.0167
92	1	86	0.124	1	0.0061
92	2	83.7	0.317	20	0.0251
92	3	85	0.239	19	0.0191
92	4	88.1	0.35	24	0.012
92	5	88.3	0.417	20	0.0187
92	6	89.4	0.319	1	0.0066
92	7	90.9	0.155	23	0.006
92	8	92	0.13	12	0.0144

92	9	90.8	0.304	22	0.0095
92	10	92	0.126	7	0.0054
92	11	91.9	0.167	21	0.0115
92	12	92.6	0.122	21	0.0098
93	1	92.5	0.086	0	0.0188
93	2	91.8	0.276	22	0.0148
93	3	90.4	0.102	23	0.0076
93	4	92.2	0.405	1	0.0084
93	5	93.4	0.282	2	0.009
93	6	94.1	0.274	1	0.0082
93	7	94.4	0.21	2	0.0111
93	8	94.1	0.145	1	0.0056
93	9	95.1	0.144	2	0.0049
93	10	95.3	0.061	15	0.0122
93	11	94	0.087	15	0.0069
93	12	94.5	0.202	5	0.0137
94	1	94.8	0.264	0	0.015
94	2	93.4	0.163	3	0.0138
94	3	93	0.147	22	0.01
94	4	93	0.251	22	0.0098
94	5	94.4	0.406	1	0.0038
94	6	94.7	0.117	0	0.011
94	7	95.2	0.239	23	0.006
94	8	95	0.4	1	0.009
94	9	96.4	0.202	1	0.0079
94	10	96	0.298	1	0.0115
94	11	95.9	0.294	24	0.0064
94	12	95.5	0.258	22	0.014
95	1	96	0.144	0	0.0071
95	2	96.2	0.415	21	0.0078
95	3	96	0.333	22	0.0164
95	4	96	0.099	2	0.0115
95	5	96.6	0.058	24	0.0063
95	6	96.5	0.335	23	0.0083
95	7	96.8	0.027	5	0.0051
95	8	97	0.14	24	0.0149
95	9	97.1	0.207	2	0.0159
95	10	97.1	0.283	23	0.0191
95	11	97.2	0.154	1	0.0055
95	12	96.7	0.14	19	0.0055
96	1	97	0.146	14	0.0143
96	2	98.1	0.27	10	0.0158
96	3	97.8	0.169	21	0.0081

96	4	98.1	0.185	20	0.0089
96	5	97.8	0.056	22	0.0091
96	6	97.8	0.077	0	0.0097
96	7	97.5	0.02	2	0.0082
96	8	97.2	0.165	2	0.0062
96	9	98	0.289	3	0.0073
96	10	97.2	0.256	3	0.0069
96	11	96.3	0.189	24	0.0072
96	12	97.1	0.101	18	0.0036
97	1	97.6	0.225	23	0.0165
97	2	97.8	0.201	23	0.0117
97	3	98	0.218	22	0.0065
97	4	97.8	0.041	22	0.0089
97	5	97.8	0.214	22	0.0102
97	6	98.3	0.195	23	0.0155
97	7	97.8	0.193	22	0.0043
97	8	98.7	0.133	22	0.0202
97	9	98	0.124	21	0.0084
97	10	98.3	0.056	22	0.008
97	11	97.4	0.202	20	0.0058
97	12	97.6	0.05	16	0.0111
98	1	97.3	0.248	1	0.0147
98	2	97.9	0.17	23	0.0135
98	3	98.2	0.02	16	0.0114
98	4	96.8	0.039	1	0.0329
98	5	94.8	0.131	0	0.0369
98	6	95	0.329	2	0.0142
98	7	95.4	0.311	23	0.017
98	8	95.4	0.245	5	0.0217
98	9	95.7	0.247	21	0.0097
98	10	96.3	0.116	20	0.0142
98	11	95.9	0.164	23	0.0092
98	12	94.9	0.243	1	0.0172
99	1	92.1	0.24	22	0.0163
99	2	92.7	0.229	21	0.0205
99	3	92.4	0.312	23	0.0175
99	4	93.4	0.384	21	0.0081
99	5	94	0.51	24	0.0364
99	6	94.5	0.24	1	0.0365
99	7	95.3	0.317	6	0.0125
99	8	93.1	0.494	20	0.1183
99	9	90.9	0.571	2	0.0177
99	10	90.3	0.283	23	0.0133

99	11	89.8	0.312	22	0.0065
99	12	87.8	0.156	23	0.0095
0	1	89.6	0.265	2	0.0068
0	2	88.3	0.234	24	0.0175
0	3	87	0.127	2	0.0125
0	4	87.6	0.256	1	0.0068
0	5	85.4	0.316	3	0.0222
0	6	83.9	0.11	18	0.0591
0	7	83.8	0.191	24	0.0053
0	8	85	0.186	22	0.0084
0	9	83.7	0.124	21	0.0049
0	10	85.7	0.211	23	0.0037
0	11	83.7	0.452	23	0.0072
0	12	85.2	0.251	3	0.0102
1	1	85.2	0.038	1	0.0064
1	2	88	0.156	22	0.0237
1	3	90.3	0.246	2	0.0102
1	4	86	0.508	2	0.0171
1	5	86.5	0.147	0	0.0266
1	6	87.4	0.396	3	0.0048
1	7	87.7	0.382	2	0.0129
1	8	87.2	0.165	15	0.1052
1	9	86.9	0.276	4	0.0055
1	10	85.9	0.32	20	0.017
1	11	87.8	0.341	0	0.0159
1	12	88.3	0.086	22	0.0114
2	1	83.7	0.117	1	0.0104
2	2	87.6	0.154	23	0.0059
2	3	87.2	0.19	22	0.0066
2	4	86.9	0.334	4	0.0109
2	5	86.9	0.268	7	0.0157
2	6	87.6	0.262	1	0.01
2	7	87.6	0.342	0	0.0101
2	8	83.7	0.427	0	0.0173
2	9	85.3	0.321	3	0.0152
2	10	86.3	0.325	2	0.0205
2	11	86.3	0.592	5	0.0234
2	12	85.4	0.054	24	0.0068
3	1	86.7	0.181	24	0.0097
3	2	86.2	0.146	24	0.0049
3	3	87.3	0.079	20	0.0097
3	4	85.9	0.103	21	0.0099
3	5	86.6	0.164	22	0.0101

3	6	84	0.29	5	0.0099
3	7	85.5	0.102	5	0.011
3	8	85.9	0.404	0	0.0055
3	9	87.5	0.359	3	0.0112
3	10	87	0.144	20	0.0152
3	11	80.8	0.458	20	0.0354
3	12	87	0.263	3	0.0102
4	1	85	0.121	6	0.0251
4	2	88.6	0.239	3	0.0101
4	3	90.1	0.149	23	0.0127
4	4	91.1	0.16	2	0.0049
4	5	92.1	0.247	3	0.0054
4	6	91.7	0.173	24	0.0136
4	7	92.4	0.211	0	0.0038
4	8	90.5	0.328	2	0.0103
4	9	92.7	0.315	2	0.009
4	10	94.2	0.303	2	0.0082
4	11	92.6	0.253	1	0.0127
4	12	93.6	0.142	1	0.0192
5	1	90.2	0.249	19	0.0337
5	2	91.6	0.21	0	0.0126
5	3	92	0.232	0	0.006
5	4	92.9	0.258	1	0.0068
5	5	92.8	0.208	3	0.0123
5	6	93.1	0.431	24	0.0141
5	7	93.5	0.291	1	0.0255
5	8	91.4	0.23	0	0.0157
5	9	90.6	0.376	1	0.0138
5	10	93	0.29	2	0.0079
4	11	92.6	0.253	1	0.0127
4	12	93.6	0.142	1	0.0192
6	1	94	0.21	0	0.0093
6	2	95.6	0.041	0	0.0078
6	3	96.1	0.25	24	0.0066
6	4	96.9	0.227	6	0.0123
6	5	97.4	0.151	2	0.0119
6	6	97.5	0.3	4	0.0064
6	7	96.9	0.37	3	0.0099
6	8	97.3	0.36	3	0.0043
6	9	97.3	0.379	3	0.0025
6	10	97.8	0.274	0	0.0077
6	11	98	0.296	1	0.0175
6	12	97.5	0.355	1	0.0092

7	1	97.9	0.329	3	0.01
7	2	98	0.175	1	0.0079
7	3	98.4	0.245	2	0.023
7	4	99.1	0.18	24	0.0142
7	5	99.5	0.341	3	0.0088
7	6	99.1	0.127	0	0.0131
7	7	99.1	0.269	2	0.0081
7	8	99.1	0.256	2	0.0043
7	9	99.5	0.144	23	0.0056
7	10	99.9	0.145	4	0.0214
7	11	99.2	0.33	2	0.0073
7	12	99.6	0.256	2	0.0076

THULE CR COUNT RATE RESULTS FROM DFT

Years	Months	%Monthly mean CR	%Diurnal amplitude	Diurnal phase-time	Dispersion
81	1	88.3	0.048	18	0.0085
81	2	87.8	0.144	17	0.0135
81	3	87.6	0.191	19	0.0102
81	4	85.2	0.073	24	0.0165
81	5	85.8	0.281	20	0.0149
81	6	87.3	0.115	16	0.0209
81	7	88.3	0.154	18	0.0087
81	8	87.7	0.129	18	0.016
81	9	89.3	0.121	19	0.0188
81	10	84.6	0.373	18	0.0252
81	11	85.9	0.186	18	0.0134
81	12	87.6	0.045	18	0.0082
82	1	90.4	0.264	20	0.0204
82	2	87.2	0.128	19	0.0101
82	3	90	0.285	17	0.0509
82	4	89.3	0.112	18	0.0112
82	5	91	0.141	20	0.0098
82	6	88.3	0.17	21	0.0813
82	7	85.8	0.122	23	0.0153

82	8	82.4	0.202	20	0.0245
82	9	81.6	0.244	17	0.0214
82	10	83.6	0.156	13	0.0091
82	11	84	0.241	19	0.0239
82	12	83	0.166	2	0.0152
83	1	83.8	0.207	21	0.0127
83	2	87	0.144	12	0.0164
83	3	86.8	0.047	15	0.0136
83	4	87.7	0.04	15	0.0105
83	5	85.7	0.313	16	0.0237
83	6	86.7	0.119	21	0.0096
83	7	88.2	0.177	21	0.0214
83	8	87.9	0.173	22	0.0108
83	9	89.7	0.191	19	0.0118
83	10	89.5	0.019	18	0.0105
83	11	90.9	0.108	18	0.0141
83	12	90.5	0.218	19	0.0113
84	1	90.7	0.154	20	0.0147
84	2	90.9	0.258	14	0.1171
84	3	89.8	0.135	19	0.0145
84	4	89.6	0.045	21	0.0161
84	5	87.6	0.207	18	0.0193
84	6	89.3	0.274	19	0.0229
84	7	89.6	0.172	21	0.0143
84	8	90.9	0.138	20	0.0202
84	9	91.4	0.298	20	0.018
84	10	91.8	0.056	14	0.0079
84	11	91.6	0.169	20	0.0082
84	12	92.1	0.137	21	0.0108
85	1	91.4	0.17	22	0.0094
85	2	92.7	0.106	18	0.0058
85	3	92.8	0.14	20	0.0253
85	4	94.6	0.137	18	0.0192
85	5	95.2	0.223	21	0.0165
85	6	95.9	0.17	20	0.0108
85	7	95.4	0.262	20	0.0089
85	8	95.4	0.19	21	0.0127
85	9	96.1	0.136	21	0.015
85	10	97	0.306	22	0.0325
85	11	97.3	0.248	20	0.015
85	12	96.3	0.133	16	0.0115
86	1	97.4	0.046	19	0.0124
86	2	95.6	0.133	22	0.0164

86	3	95.1	0.1	8	0.0202
86	4	97.6	0.146	18	0.0141
86	5	99.1	0.175	19	0.0072
86	6	99	0.084	20	0.0157
86	7	98.9	0.383	22	0.0091
86	8	99.1	0.216	23	0.0133
86	9	99.6	0.088	22	0.0093
86	10	100	0.055	14	0.0089
86	11	98.5	0.085	13	0.0091
86	12	99.6	0.008	11	0.0107
87	1	100.7	0.11	15	0.0061
87	2	102.1	0.15	19	0.014
87	3	101.3	0.124	16	0.0116
87	4	101.5	0.184	17	0.009
87	5	101.2	0.099	17	0.0111
87	6	98.9	0.183	21	0.0124
87	7	98.5	0.087	19	0.0101
87	8	98	0.232	18	0.0199
87	9	96.7	0.124	22	0.0129
87	10	96.8	0.112	18	0.0038
87	11	95.9	0.115	13	0.0139
87	12	96.2	0.056	3	0.0073
88	1	94.1	0.176	21	0.0188
88	2	94.3	0.156	21	0.0093
88	3	94.7	0.114	20	0.016
88	4	93.7	0.098	10	0.0131
88	5	94.2	0.208	20	0.0226
88	6	93.8	0.291	18	0.0108
88	7	92.5	0.074	20	0.0145
88	8	91.7	0.298	18	0.02
88	9	91.7	0.136	19	0.0068
88	10	91.2	0.166	17	0.0159
88	11	90.7	0.051	21	0.01
88	12	89.8	0.165	20	0.0099
89	1	87.4	0.076	10	0.0096
89	2	85.7	0.126	23	0.0105
89	3	82.6	0.276	18	0.0239
89	4	82.9	0.195	21	0.0111
89	5	81.6	0.4	17	0.0364
89	6	82.1	0.292	21	0.0552
89	7	83.8	0.159	16	0.0068
89	8	84.4	0.225	9	0.0091
89	9	80.5	0.387	18	0.013

89	10	81.3	0.277	22	0.017
89	11	79	0.244	21	0.0079
89	12	80.2	0.098	18	0.009
90	1	82	0.138	22	0.0121
90	2	83.6	0.126	18	0.0138
90	3	81.8	0.246	20	0.0127
90	4	80.9	0.113	19	0.0121
90	5	79.8	0.273	21	0.0143
90	6	78.4	0.236	19	0.0162
90	7	81.4	0.112	19	0.0189
90	8	80.9	0.183	20	0.0131
90	9	82.8	0.081	16	0.0085
90	10	84.1	0.095	21	0.0125
90	11	84.9	0.139	19	0.0178
90	12	83.6	0.096	3	0.0122
91	1	87.2	0.187	20	0.0141
91	2	87.2	0.214	19	0.0126
91	3	82	0.289	19	0.0159
91	4	82.1	0.145	19	0.0097
91	5	83.3	0.506	1	0.032
91	6	73.9	0.435	18	0.0605
91	7	75.9	0.25	19	0.031
91	8	79.4	0.145	19	0.016
91	9	83.3	0.069	19	0.0123
91	10	84.5	0.145	3	0.008
91	11	85.8	0.343	18	0.0252
91	12	85.2	0.11	17	0.0114
92	1	87.9	0.112	19	0.0128
92	2	85.4	0.405	18	0.0372
92	3	86.1	0.278	18	0.0166
92	4	88.5	0.219	18	0.0201
92	5	89.9	0.49	18	0.0365
92	6	91.1	0.176	19	0.0129
92	7	92.9	0.098	22	0.0091
92	8	93.7	0.159	16	0.0136
92	9	92.2	0.179	20	0.0193
92	10	93.7	0.02	15	0.0155
92	11	93.9	0.233	18	0.0242
92	12	94.9	0.105	18	0.0096
93	1	93.3	0.254	19	0.0133
93	2	93.2	0.415	18	0.0267
93	3	91.4	0.098	18	0.0162
93	4	93.2	0.208	18	0.0107

93	5	93.9	0.238	21	0.0053
93	6	94.7	0.182	21	0.0099
93	7	95.3	0.306	19	0.013
93	8	95.3	0.066	19	0.0097
93	9	95.9	0.146	19	0.0084
93	10	95.7	0.123	21	0.0275
93	11	95.5	0.102	17	0.0088
93	12	95.2	0.207	21	0.0157
94	1	94.7	0.164	15	0.0199
94	2	93	0.184	21	0.0282
94	3	93.7	0.071	16	0.0086
94	4	93.9	0.19	19	0.0207
94	5	95	0.226	20	0.0129
94	6	94.6	0.199	20	0.0285
94	7	95.5	0.125	18	0.0151
94	8	95.5	0.22	19	0.0145
94	9	96.1	0.066	16	0.0123
94	10	95.7	0.237	20	0.007
94	11	95.8	0.155	20	0.0188
94	12	96.5	0.246	18	0.0145
95	1	96.4	0.262	18	0.0114
95	2	96.7	0.165	16	0.0141
95	3	96.5	0.324	16	0.0192
95	4	96.6	0.06	11	0.0235
95	5	97.5	0.06	11	0.0212
95	6	97	0.194	19	0.006
95	7	97.3	0.085	9	0.0226
95	8	97.2	0.194	18	0.0122
95	9	97.6	0.169	6	0.0247
95	10	97.3	0.224	18	0.0262
95	11	97.5	0.15	21	0.0122
95	12	97.2	0.07	17	0.0085
96	1	97.7	0.065	8	0.005
96	2	98.1	0.148	11	0.0183
96	3	98.6	0.197	16	0.0146
96	4	97.9	0.112	14	0.0103
96	5	97.5	0.069	16	0.0122
96	6	97.8	0.103	20	0.009
96	7	97.8	0.082	15	0.0065
96	8	97.4	0.042	5	0.0198
96	9	98.3	0.053	1	0.017
96	10	97.2	0.222	3	0.0158
96	11	96.6	0.06	7	0.0092

96	12	97.5	0.099	16	0.0108
97	1	97.6	0.138	22	0.0477
97	2	98.1	0.139	18	0.0144
97	3	98.3	0.033	13	0.0122
97	4	97.5	0.042	12	0.01
97	5	97.8	0.089	17	0.0077
97	6	NaN	NaN	NaN	NaN
97	7	NaN	NaN	NaN	NaN
97	8	NaN	NaN	NaN	NaN
97	9	NaN	NaN	NaN	NaN
97	10	NaN	NaN	NaN	NaN
97	11	NaN	NaN	NaN	NaN
97	12	NaN	NaN	NaN	NaN
98	1	98.3	0.096	9	0.016
98	2	98.5	0.092	21	0.0092
98	3	99.3	0.034	15	0.009
98	4	97.9	0.032	18	0.0186
98	5	94.7	0.298	19	0.0474
98	6	95.1	0.336	20	0.0214
98	7	95.8	0.214	19	0.0191
98	8	95.7	0.082	15	0.0061
98	9	95.9	0.278	17	0.0184
98	10	96.4	0.161	16	0.0113
98	11	96.1	0.093	20	0.0147
98	12	95	0.159	20	0.0163
99	1	92.5	0.52	17	0.0405
99	2	93.2	0.197	18	0.0191
99	3	92.9	0.191	17	0.0218
99	4	93.6	0.292	18	0.0148
99	5	94	0.223	19	0.0154
99	6	95.4	0.176	20	0.0086
99	7	96	0.25	2	0.0169
99	8	93.4	0.105	15	0.009
99	9	91.9	0.253	20	0.0141
99	10	90.8	0.192	18	0.0166
99	11	90.1	0.256	17	0.0153
99	12	88.5	0.168	17	0.0171
0	1	89.7	0.097	19	0.0146
0	2	88.3	0.103	19	0.0044
0	3	86.9	0.063	20	0.0069
0	4	87.5	0.183	18	0.0156
0	5	85.5	0.049	11	0.0232
0	6	84.3	0.204	18	0.0232

0	7	84.2	0.277	17	0.0232
0	8	85.4	0.182	17	0.0139
0	9	85.7	0.108	23	0.0118
0	10	87.2	0.125	16	0.0137
0	11	86	0.263	18	0.0119
0	12	86.9	0.199	21	0.0086
1	1	86.6	0.129	18	0.0104
1	2	88.3	0.099	16	0.0092
1	3	90.3	0.191	21	0.0124
1	4	86	0.325	19	0.0164
1	5	87	0.247	20	0.0267
1	6	88.7	0.249	21	0.0068
1	7	88.9	0.09	24	0.0061
1	8	87.2	0.187	21	0.0071
1	9	87.6	0.22	18	0.0123
1	10	86.2	0.285	18	0.0224
1	11	87.3	0.465	20	0.0194
1	12	88.3	0.154	18	0.0079
2	1	84.4	0.135	18	0.0058
2	2	87.9	0.127	19	0.0057
2	3	88	0.181	18	0.0218
2	4	88	0.103	20	0.0068
2	5	87	0.194	19	0.026
2	6	88.1	0.185	19	0.005
2	7	88.5	0.173	21	0.0093
2	8	84.5	0.186	19	0.0192
2	9	86.1	0.196	22	0.013
2	10	86.9	0.048	4	0.0049
2	11	86.5	0.352	6	0.0228
2	12	86.4	0.144	16	0.0082
3	1	86.6	0.14	19	0.0071
3	2	86.6	0.08	19	0.0058
3	3	87.3	0.081	15	0.0032
3	4	86.1	0.233	18	0.0103
3	5	86.6	0.168	18	0.0092
3	6	84.5	0.256	3	0.0127
3	7	86.2	0.05	2	0.0069
3	8	86.1	0.113	21	0.0103
3	9	87.6	0.182	23	0.0078
3	10	87.8	0.172	19	0.0191
3	11	81	0.532	18	0.0648
3	12	86.4	0.346	19	0.0053
4	1	85.1	0.055	7	0.0091

4	2	89	0.115	20	0.0115
4	3	90.3	0.205	18	0.0063
4	4	90.9	0.188	19	0.0053
4	5	92.4	0.216	20	0.0052
4	6	92.2	0.206	18	0.0125
4	7	92.6	0.204	19	0.0068
4	8	90.6	0.292	20	0.01
4	9	92.7	0.192	21	0.007
4	10	94.2	0.25	19	0.0054
4	11	92.5	0.234	19	0.0088
4	12	92.3	0.219	22	0.0071
5	1	89.2	0.214	17	0.0123
5	2	91.1	0.164	19	0.0151
5	3	90.8	0.156	20	0.0071
5	4	91.8	0.184	19	0.0053
5	5	92.6	0.233	20	0.0173
5	6	93.3	0.353	19	0.007
5	7	93.7	0.222	19	0.0043
5	8	91.8	0.22	19	0.0063
5	9	91	0.357	21	0.0093
5	10	92	0.296	21	0.0039
5	11	94.3	0.184	19	0.0098
5	12	94.4	0.298	20	0.0081
6	1	95	0.185	17	0.007
6	2	96.5	0.039	5	0.0069
6	3	96.8	0.304	18	0.0175
6	4	97.7	0.04	2	0.007
6	5	97.7	0.16	20	0.0079
6	6	97.9	0.15	21	0.0061
6	7	97.1	0.219	21	0.0054
6	8	97.4	0.156	0	0.0178
6	9	97.5	0.2	22	0.0076
6	10	98.3	0.202	20	0.005
6	11	97.4	0.191	21	0.0036
6	12	96.7	0.149	21	0.0078
7	1	97.4	0.202	20	0.0081
7	2	97.2	0.08	20	0.0037
7	3	98.2	0.147	18	0.0082
7	4	98.4	0.109	20	0.008
7	5	99.3	0.172	21	0.0041
7	6	99.2	0.195	19	0.0197
7	7	99.6	0.175	20	0.007
7	8	99.4	0.189	20	0.006

7	9	100.2	0.099	19	0.0081
7	10	100	0.165	21	0.0052
7	11	100.3	0.216	20	0.0067
7	12	99.8	0.251	19	0.0132